We thank the reviewers for their careful reviews and helpful comments. The manuscript has been revised accordingly and our point-by-point responses are provided below. (Reviewers' comments are in italic and the responses in standard font).

Reviewer #1

The authors present a 4-mode modal aerosol model (MAM4) by introducing a primary carbon mode to the existing 3-mode version of MAM (MAM3) in the Community Atmosphere Model version 5 (CAM5). They further design two sets of sensitivity experiments, one to change the aging properties of primary carbon and another to change model resolution, to investigate the potential improvement of atmospheric black carbon simulation. The paper is well written. I recommend publishing the paper on ACP after the authors make some minor modifications.

General Remarks:

My only concern is the performance of MAM4 relative to MAM3. The authors evaluate BC results simulated from MAM3 and two sets of sensitivity experiments of MAM4 using various aircraft measurements. With the exception of high latitudes of the Northern Hemisphere, the performance of MAM4 BC simulation over global broad coverage is deteriorated, overestimating BC compared to measurements.
Over the North Pole region, MAM4 BC is still underestimated and the authors suggest further improvements on in-cloud scavenging and vertical transport in convective cloud and on emissions. These actions, while they can potentially improve BC over North Pole, are very likely to further downgrade BC simulation outside North Pole regions.

Reply: We agree with the reviewer that the primary goal of MAM4 is to improve the BC/POM simulation in remote places away from the source regions by treating the aging process of BC/POM that is neglected in MAM3. However, because the current model is calibrated for MAM3, running the model with MAM4 results in the overestimation of BC concentrations in the free troposphere in the regions evaluated in this study (e.g., remote Pacific during the HIPPO campaign, and tropics, NH subtropics and NH mid-latitudes during the AVE-Houston, CR-AVE, and TC4 campaigns).

We suggest a potential further improvement of in-cloud scavenging and convective transport of aerosols in the manuscript. As shown in H. Wang et al. (2013), with a unified treatment of in-cloud scavenging and vertical transport in convective clouds, the overestimation of BC in the free troposphere in the remote regions (e.g., over the Pacific) is significantly reduced, due to the inclusion of secondary activation and thus more efficient scavenging of aerosols in convective clouds. Meanwhile, H. Wang et al. (2013) found that the liquid cloud fraction in the NH mid- and high latitudes is too high, which leads to too efficient scavenging of BC during it transport from the NH mid-latitudes. By modifying the treatment of liquid cloud fraction in cloud scavenging parameterization for the NH high latitudes, H. Wang et al. (2013) gave a much better simulation of near-surface BC and other aerosol species in the Arctic than simulation from the standard CAM5.

We also suggest a further improvement on aerosol emissions. As pointed out by Stohl et al. (2013), BC emissions in the NH high latitudes are underestimated and gas flaring emissions are omitted in the IPCC AR5 emission inventory used in CAM5 simulations. We anticipate that the low BC bias in the Arctic can be reduced by improving the emission inventory. We note that improvements in emissions in the NH high latitudes (in and near the Arctic) would not necessarily downgrade the simulation outside North Pole regions.

A more recent improved model treatment in the resuspension of aerosols from evaporated raindrops, releasing aerosol particles to the coarse mode instead of their originating mode upon complete evaporation of raindrops (Easter et al., 2015, personal communication), has shown a significant impact on the vertical distribution of aerosols, including large reductions in mid- and upper tropospheric BC and POM.

The manuscript has been revised in Section 5 to include the discussion above.

Specific comments:

1. Page 8342 lines 22-23: Overestimating BC over Pacific region is a common problem for many global aerosol models. Changing emission based on various available emission inventories cannot solve the problem.

Reply: As discussed in the manuscript, the overestimation of BC over the Pacific can be mitigated by the improved treatment of in-cloud scavenging and vertical transport in convective clouds, as shown in H. Wang et al. (2013). Other model improvements in cloud processing of aerosols (e.g., Easter et al., 2015, personal communication) would also help reduce the high bias. The low BC bias in the Arctic is much reduced with MAM4, although BC concentrations are still lower than observations. Stohl et al. (2013) pointed out that BC emissions in the NH high latitudes are underestimated in the AR5 emission inventory. We anticipate that the low BC bias in the Arctic can also be reduced by improving the BC emissions.

2. Page 8343 line 22: Add Bian et al., 2013 alone with Wang et al., 2013.

Reply: Done.

3. Page 8343 line 23: Add Jiao et al., 2014 after "dry and wet deposition".

Reply: Done.

4. Page 8344 line 1: Add "and II" and "Phase I".

Reply: Done.

5. Page 8344 line 1: Add "Samset et al. 2014" after "Schwarz et al., 2010".

Reply: Done.

6. Page 8344 line 11: Add "nitrate" after "sulfate".

Reply: Currently MAM does not treat nitrate. To avoid misunderstanding, we prefer to remain the original wording, "(e.g., sulfate)".

7. Page 8344 lines 15-16: Does "its" refer to BC's? If yes, why is "BC's" absorption of sunlight enhanced significantly since soluble species, typically sulfate and nitrate, have less absorption than BC's?

Reply: Yes, "its" refers to BC's. We have explained this more clearly in terms of the lensing effect for the shell-core treatment (Jacobson 2001, 2003), and in terms of increasing the cross section of the absorbing material for the volume mixing treatment (Adachi et al., 2010). We've also added a paragraph in section 2.3 on the volume mixing treatment used in MAM4.

8. Page 8345 lines 19-24: If these are the reasons for the underestimation of BC at high latitude of Northern Hemisphere, then how do the authors explain the overestimation of BC over other regions?

Reply: In the manuscript we describe the CAM5 (with MAM3) low bias for near-surface BC concentrations in the Arctic, and review previous studies that attribute the bias to emissions, wet scavenging parameterization, and model resolution. The overestimation of BC occurs in the upper troposphere in other regions (e.g., remote Pacific), which is another important model bias. We believe that this high BC bias in the upper troposphere is largely due to the treatment of vertical transport and wet removal in convective clouds. A revised treatment of these processes in H. Wang et al. (2013), which included secondary activation in convective updrafts, noticeably reduced this upper-troposphere high bias with MAM3. This revised treatment was not used in our simulations because it is not included in the standard CAM5 code yet.

9. Page 8346 lines 10-12: How does aerosol affect convective cloud?

Reply: In CAM5, aerosol does not affect the microphysical processes of convective clouds. We have made it clear in the revised manuscript.

10. Page 8348 lines 8-11: Do the authors use different hygroscopicity for fossil fuel POM and biomass burning or use the same value for both?

Reply: The hygroscopicity of POM from fossil fuel and biomass burning sources is set to be the same in this study. We have made it clear in the revised manuscript.

11. Page 8349 lines 13-15, Page 8350 lines 3-4, and Figures 6-14: How large is the inter-annual variation of BC over the comparison regions? The current approach of the

comparison implies that the inter-annual change of BC is very small.

Reply: As described in Section 3, our set 1 experiments were conducted using the present-day (i.e., year 2000) climate forcing conditions for 11 years with the last 10-year results used for analysis. It is not an AMIP-type configuration so a specific model year does not represent any particular calendar year. The 10-year average is viewed as an ensemble mean, representing the model's present-day climatology. Ideally the model climatology should be evaluated against the corresponding observational climatology. However, the field campaigns were conducted in a particular time period and such a comparison is not feasible. Our purpose is to provide the model climatology from the sensitivity study and use the aircraft measurements as a reference, and acknowledge that the observation represents a particular year while the model results are climatology. Therefore, the inter-annual variation of BC due to meteorology and/or forcings (e.g., aerosol emissions) cannot be quantified from such experiments. Other than these factors, the inter-annual variation of modeled BC due to natural variability (i.e., BC difference among different years of 10-year climatology) is quantified to be very small, as indicated by the standard deviations of BC/POM budget terms about the 10-year mean in Tables 2 and 3 for the set 1 experiments (added in the revised manuscript).

By contrast, our set 2 experiments are nudged toward the year of 2009 meteorology. The differences in BC from MAM4L8 of set 1 and MAM4R1 of set 2 experiments are due to differences in their meteorology (winds, clouds, and precipitation), which include the differences between a 10 year average (or ensemble) and a single year, as well as the differences between the free-running model's meteorology and the nudged model's meteorology (which is very close to the reanalysis).

We have revised the manuscript to clarify the model-to-observation comparison strategy.

12. Page 8354 line 19: Add Bian et al., 2013 after Ma et al., 2013.

Reply: Done.

13. Figure 6: Why is MAM3 result not shown on the figure?

Reply: The MAM3 result is already shown in Tilmes et al. (2015). We have added a sentence to direct readers to Tilmes et al. (2015) for MAM3 result.

14. Figures 7-12: How are the model results sampled spatially and temporally when they are compared with observations?

Reply: The model results are sampled in the same way as Liu et al. (2012): Simulated profiles are averaged over the locations on the map and the indicated month of respective field campaigns (in Figures 7-12). This sentence has been added to the figure captions.

Technique corrections:

Page 8344 lines 4-5: Change "compared" to "comparable" and delete "the models tend to be in better agreement".

Reply: Done.

We thank the reviewers for their careful reviews and helpful comments. The manuscript has been revised accordingly and our point-by-point responses are provided below. (Reviewer's comments are in italic and the responses in standard font).

Reviewer #2

The manuscript presents MAM4, an extended version of the three-mode MAM3 aerosol scheme incorporating an additional externally-mixed mode for primary carbonaceous aerosol. This allows it to represent the delayed transition to the hydrophilic state via ageing processes, but without the full complexity of the seven-mode MAM7 scheme. Improvements to the aerosol distribution are well demonstrated, and also compared with those from increasing model resolution.
The manuscript is well presented, based on sound methodology and shows clear results. Subject to the comments below, I would certainly recommend it for publication in GMD.

1 General comments:

Since MAM4 is positioned between MAM3 and MAM7 in terms of its complexity, it is a pity that it is only compared against the former. An additional run with MAM7 in set 1 would demonstrate how much of the improvement in MAM7 is achieved by MAM4 with its lower computational cost.

Reply: We conducted an experiment with MAM7. Since MAM4's primary carbon mode is the same as that in MAM7, the difference in BC and POM simulations between MAM4 and MAM7 is negligible. Thus we don't include the results of MAM7 in the comparison. We have made this clear in the model experiment section 3 and conclusion section 5.

For the set 2 experiments, the model is constrained by the YOTC analysis. Does this cover the time period of all the observational campaigns used, in order that these evaluations can be performed on the correct year? If not, how do the authors deal with interannual meteorological variability when comparing simulations for one year with observations for another?

Reply: We agree with the reviewer that the interannual meteorological variability is not accounted for in this evaluation strategy. Unfortunately the YOTC analysis is only available between May 2008 and May 2010, while some field campaigns used in this study were conducted in other years (e.g., NASA ARCTAS and NOAA ARCPAC campaigns took place in April 2008). However, our purpose is to present the new improvement in MAM4 with two sets of sensitivity experiments using the same evaluation strategy as in Liu et al. (2012) for MAM3 and MAM7 to highlight the importance of the BC/POM aging process and model resolution. We have acknowledged the potential effect of interannual meteorological variability on our model-observation comparisons in the revised manuscript.

Similarly, could the authors please clarify the temporal nature of the biomass-burning emissions in particular? These are highly variable, and there is likely to be a large

difference between using climatological or hindcast-style "correct year" emissions when comparing to specific campaigns.

Reply: We agree with the reviewer that the time-dependent nature of biomass-burning emissions can affect our model-observation comparisons for specific campaigns. Our experiments are designed to be consistent with Liu et al. (2012), to highlight the importance of the BC/POM aging process and model resolution. Our set 1 experiments were conducted using the present-day (i.e., year 2000) climate forcing conditions, including aerosol emissions, instead of AMIP-type configurations. Thus the interannual variability for biomass-burning emissions is not accounted for in this study. We have acknowledged the effect of interannual variability of biomass-burning emissions on our model comparisons to specific campaigns in the revised manuscript.

We checked the interannual variability of biomass-burning emissions from GFED version 3.1 (van der Werf et al., ACP, 2010) for the time period of year 2004 to 2011. The annual fire BC plus OC emissions in boreal regions (including N. America and Russia) vary by more than a factor of 2 from 2007 with the lowest emissions to 2008 with the strongest emissions (Figure R1). However, the interannual variability of biomass burning emissions still can not account for the large difference between model simulations and observations (by more than a factor of 10 in the Arctic).

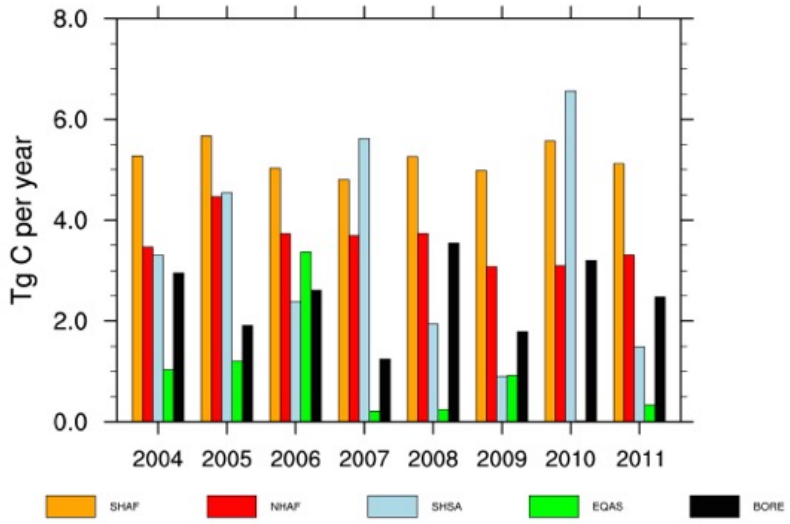

Figure R1. Annual BC plus OC emissions in different regions from 2004 to 2011 from the GFED emission inventory. SHAF: southern hemisphere Africa; NHAF: northern hemisphere Africa; SHSA: southern hemisphere southern America; EQAS: equatorial Asia; BORE: boreal region (in both N. America and Russia).

In the budget analysis presented in Section 4.2, is it possible to quantify the interannual variability in these budgets and thus to determine whether or not the differences are statistically significant?

Reply: It is a great idea and we have added the standard deviation (from the 10-year

average) in the budget analysis. We have added the standard deviations in Tables 2-3 for the set 1 experiments in the revised manuscript.

When comparing the model to the aircraft campaigns in Figures 9–12, how is the model sampled in space and time to match the observations? (Is it interpolated to the flight time and location, or are e.g. monthly means over some region used? This will affect the sampling error to be expected in the comparison.)

Reply: The model results are sampled in the same way as Liu et al. (2012): Simulated profiles are averaged over the points on the map and the indicated month of each campaign. This sentence has been added to the figure captions of Figures 7-12.

2 Detailed comments

Page 8344, lines 3–5. If the models compare better with ground-based sun photometer measurements than with satellite retrievals, doesn't this suggest that the poorer comparison with satellite might be due in part to either retrieval errors or collocation/sampling issues between models and observations, rather than deficiencies in the models?

Reply: This is indeed a possibility that certainly requires further investigation. We have added the reviewer's comments in the manuscript and call for further studies.

Page 8344, lines 6–9. Hydrophobic and water-insoluble are not quite the same thing. Insoluble materials may nevertheless be hydrophilic ("wettable") and thus act as CCN via adsorption, although this is rarely treated in models. Also, "and are not able to nucleate cloud droplets" is unnecessary – this is what "cannot serve as CCN" means.

Reply: Following the reviewer's comment, we have removed "water insoluble" and "and are not able to nucleate cloud droplets" in the revision.

Page 8345, line 20. Remove hyphen in "high latitudes" and insert "the" before "northern hemisphere".

Reply: Done.

Page 8346, line 21. Please explain how homogeneous nucleation might be affected by aerosol particles. Unlike for heterogeneous nucleation, this is not clear.

Reply: homogeneous nucleation is the spontaneous freezing of aerosol solution droplets such as sulfate aerosol. Change in the sulfate aerosol number can affect the number and size of ice crystals from homogeneous nucleation due to the competition of water vapor among the ice crystals.

We have added "of aerosol solution droplets (e.g., sulfate aerosol)" after "homogeneous

ice nucleation" in the revision.

Page 8348, line 23. Change "standard-alone" to "stand-alone" and explain what is meant by this. I presume an uncoupled atmosphere-only simulation with prescribed SST and sea ice?

Reply: We made the correction, and added "atmosphere-only simulation with prescribed SST and sea ice". Yes, this is what the "stand-alone" means.

Page 8349, line 23. By "specified dynamics" do you mean what is often referred to as "nudging" (i.e. Newtonian relaxation of model fields to the (re)analysis ones)? It's probably worth either using the term "nudging", or explaining how the technique differs.

Reply: Yes, they are the same thing. We acknowledge that there are different terminologies and have added "also known as the nudging technique" in the revised manuscript.

Page 8350, line 9. Delete "the" before "comparison".

Reply: Done.

Page 8350, line 12, and captions to Figures 2–5. "Latitude and longitudinal" is grammatically inconsistent. I'd suggest "zonal and meridional" or "latitudinal and longitudinal" instead.

Reply: Done. Changed to "latitudinal and longitudinal".

Page 8351, line 6. Although primary carbon particles may not act as CCN, they are still subject to impaction scavenging by cloud droplets, ice crystals and falling precipitation, leading to wet deposition. Please clarify if this process is included in the model or not.

Reply: Yes, the impaction scavenging by precipitating hydrometeors is included in the model. We have added the sentence "(while still subject to impaction scavenging by precipitating hydrometeors)" in the revised manuscript. The primary carbon particles are in the dry diameter range of 0.04-0.2 μm calculated from our model (Liu et al., 2012). Particles in this size range, even if hydroscopic, are less efficiently scavenged by the precipitating hydrometeors than by the in-cloud nucleation scavenging.

Page 8351, lines 28–29. Why is this of importance for aerosol–cloud interactions in particular?

Reply: Ma et al. (2015) found that increasing resolution leads to enhanced but less frequent droplet nucleation (Ma et al., 2015) due to (1) stronger subgrid vertical velocity, (2) reduced collocation of aerosols and clouds, and (3) higher aerosol concentration. We have revised the sentence for clarification. Now it reads as "The resolution sensitivity of POM/BC, as well as other aerosol particles, can contribute to the resolution sensitivity of

aerosol-cloud interactions such as the enhanced but less frequent droplet nucleation due to stronger subgrid vertical velocity, reduced collocation of aerosols and clouds, and higher aerosol concentration (Ma et al., 2015)."

Page 8352, lines 6–11. Please justify, quantify and show evidence for, the difference between SD and free-running simulations being due to a convectively less stable atmosphere.

Reply: This is from our previous study but since it is not necessary to this study, we removed the statement in the revised manuscript: "In particular, we find that the free-running CAM5 produces a convectively less stable atmosphere, which enhances the vertical transport of aerosols to higher altitudes where the aerosol lifetimes are longer."

Page 8352, lines 17–18. This gives the impression that dry deposition overtakes wet deposition as the dominant process; please clarify that wet deposition remains very much the dominant sink even at 8 mono-layers, although dry deposition becomes a larger secondary sink.

Reply: Following the reviewer's comment, we changed the sentence to "the contribution of wet deposition to the total BC sink somewhat decreases and the contribution of dry deposition increases" in the revised manuscript.

Page 8353, line 23. Inserting "absolute" before "wet removal sinks" would make it clear how these statements are consistent.

Reply: Done.

Page 8354, lines 7–8. A citation of Schwarz et al. (2013; 10.1002/2013GL057775) is probably in order for the HIPPO1–5 SP2 observations.

Reply: Done. Citation added in the revised manuscript.

Page 8355, lines 3–5. A similar attribution of excess BC in the upper troposphere to the relationship between convective transport and scavenging has been done for other models, notably HadGEM3–UKCA (Kipling et al., 2013; 10.5194/acp-13-5969-2013).

Reply: The citation has been added in the revision to "Excessive BC aloft was also found in the HadGEM3–UKCA model and was attributed to the coupling of convective transport and convective scavenging (Kipling et al., 2013)."

Pages 8356–8357, and/or Figures 9 and 11. Please add references for the aircraft campaigns used, where available.

Reply: References are added for the aircraft campaigns in the revised manuscript.

Page 8358, line 7. Should be either "which however weakens" or "which, however, weakens".

Reply: Done.

Page 8359, lines 23–25. Citation or evidence for these deficiencies in the emission inventory?

Reply: Following the reviewer's comment, we have added citations for the deficiencies of aerosol emission inventory in and around the Arctic (e.g., Stohl et al., 2013) and in East Asia (e.g., Cohan and Wang, 2014).

Page 8360, lines 14–16. Probably worth using the AR5 terminology explicitly, i.e. either "ERFaci" or "ERFari+aci", depending which this is.

Reply: Done. We changed to use the AR5 terminology $ERF_{ari+aci}$.

Table 1 caption. Try "number of ageing mono-layers set to 8", and ". . . with MAM3 is run for the comparison".

Reply: Done.

Figures 2, 4, 6, 7–12. Font sizes are very small, although this may only be due to the reduction required to fit in discussion page layout. Please check that labels etc. will be easily legible in the final paper.

Reply: Thanks for the suggestion. We will check the readability of labels etc. in these figures in the final paper.

Figure 3. Using the same colour scale for a difference plot as for the absolute burdens is confusing. Also, relative difference ((x1-x0)/x0) on a logarithmic scale seems strange. Either relative difference on a linear scale, or ratio (x1/x0) on a logarithmic scale would be easier to interpret.

Reply: We are using the same color scale for the relative differences between different MAM4 experiments and MAM3, so as to compare the differences more clearly. We prefer plotting the relative difference with logarithmic scale to capture the large spread of the relative difference for different MAM4 experiments. We think it is easy to understand.

Figures 7–12. The standard-deviation shading looks very odd, often being highly asymmetric and reaching down to zero. It's also not described in the caption of Figure 7. This is probably the result of using arithmetic standard deviations on a logarithmic scale – on such a scale, and for a quantity which roughly follows a log-normal distribution, the geometric mean and standard deviation would be more appropriate (or alternatively median and interquantile range). Including both means and medians on the plot doesn't

seem to add much, and makes them quite cluttered. I'd suggest sticking with one, and removing the other, unless some important conclusion relies on the distinction.

Reply: Following the reviewer's comment, we removed dark dashed curves for the medians in Figure 7-12. We also added the description of means and standard deviations in the caption of Figure 7.

Description and Evaluation of a New 4-Mode Version of Modal Aerosol Module (MAM4) within Version 5.3 of the Community Atmosphere Model

Xiaohong Liu[1,2], Po-Lun Ma[1], Hailong Wang[1], Simone Tilmes[3], Balwinder Singh[1], Richard C. Easter[1], Steven J. Ghan[1], and Philip J. Rasch[1]

[1] *Atmospheric Sciences and Global Change Division, Pacific Northwest National Laboratory, Richland, Washington, USA*
[2] *Now at Department of Atmospheric Science, University of Wyoming, Laramie, Wyoming, USA*
[3] *National Center for Atmospheric Research, Boulder, Colorado, USA*

Corresponding author:

Xiaohong Liu
Department of Atmospheric Science
University of Wyoming
Dept. 3038, 1000 East University Avenue
Laramie, WY 82071
Email: xliu6@uwyo.edu

Tel: (307) 766-3225
Fax: (307) 766-2635

Abstract

Atmospheric carbonaceous aerosols play an important role in the climate system by influencing the Earth's radiation budgets and modifying the cloud properties. Despite the importance, their representations in large-scale atmospheric models are still crude, which can influence model simulated burden, lifetime, physical, chemical and optical properties, and the climate forcing of carbonaceous aerosols. In this study, we improve the current 3-mode version of modal aerosol module (MAM3) in the Community Atmosphere Model version 5 (CAM5) by introducing an additional primary carbon mode to explicitly account for the microphysical ageing of primary carbonaceous aerosols in the atmosphere. Compared to MAM3, the 4-mode version of MAM (MAM4) significantly increases the column burdens of primary particulate organic matter (POM) and black carbon (BC) by up to 40% in many remote regions, where in-cloud scavenging plays an important role in determining the aerosol concentrations. Differences in the column burdens for other types of aerosol (e.g., sulfate, secondary organic aerosols, mineral dust, sea salt) are less than 1%. Evaluating the MAM4 simulation against in situ surface and aircraft observations, we find that MAM4 significantly improves the simulation of seasonal variation of near-surface BC concentrations in the polar regions, by increasing the BC concentrations in all seasons and particularly in cold seasons. However, it exacerbates the overestimation of modeled BC concentrations in the upper troposphere in the Pacific regions. The comparisons suggest that, to address the remaining model POM and BC biases, future improvements are required related to (1) in-cloud scavenging and vertical transport in convective clouds and (2) emissions of anthropogenic and biomass burning aerosols.

1. Introduction

Atmospheric aerosols from natural and anthropogenic sources play an important role in the climate system. In spite of extensive studies in the past several decades, radiative forcing of atmospheric aerosols is still associated with large uncertainties according to the Intergovernmental Panel of Climate Change Assessment Reports (Forster et al., 2007; Myhre et al., 2013). The large uncertainty of aerosol radiative forcing among global climate models (GCMs) reflects the diversity in treatments of aerosol properties and processes in GCMs. A multitude of processes influence aerosols in the atmosphere, which include emission, nucleation, coagulation, gas-phase and aqueous chemical reactions, dry deposition, gravitational settling, and wet scavenging by clouds and precipitation. These processes determine the burden and lifetime of aerosols, particle size distribution, mixing state, and thus the radiative forcing of aerosols on the climate (Textor et al., 2006; Schulz et al., 2006; Quaas et al., 2009). Furthermore, the burden and size distribution of aerosols control their surface area density and thereby influence heterogeneous chemistry, which can then induce chemical effects such as extended methane lifetime (Tilmes et al., 2015).

Primary carbonaceous aerosols are produced from the incomplete combustion of fossil and biomass fuels, and are one of the most important types of aerosol in the atmosphere. Most models tend to speciate the mass of carbonaceous aerosols into a light-absorbing component (black carbon, BC) and a purely-scattering component (particulate organic matter, POM). BC has a strong warming effect, second only to carbon dioxide on the climate system, with the industrial-era (1750 to 2005) direct radiative forcing of +0.71 W m^{-2} with 90% uncertainty bounds of (+0.08, +1.27) W m^{-2} (Bond et al., 2013).

Once emitted into the atmosphere, BC can be transported to the polar regions far from distant sources (e.g., Bian et al., 2013; H. Wang et al., 2013), and deposited on the surface of snow and sea ice by dry and wet deposition (e.g., Jiao et al., 2014). BC-in-snow can absorb solar radiation efficiently, heat the snowpack, and induce a positive feedback on the surface albedo (Hansen and Nazarenko, 2004; Jacobson, 2004; Hansen et al., 2005; Flanner et al., 2007, 2009, 2012).

Although climatologically important, BC is still not simulated well by GCMs in many regions. For example, high bias of BC concentrations in the upper troposphere in the tropics and subtropics exists in almost all the global models participating in the AeroCom Phase I and Phase II intercomparison (Koch et al., 2009; Schwarz et al., 2010; Samset et al., 2014), while low BC bias in the lower atmosphere by over a factor of 10 exists in the polar regions. The aerosol absorption optical depth also tends to be biased low in GCMs compared to satellite observations (Koch et al., 2009), although compares better to ground-based sun photometers (Kinne et al., 2006). Note that differences between satellite retrievals and ground-based observations can be attributed to collocation/sampling and/or retrieval errors, but require further investigation.

REaster 12/28/2015 5:01 PM
Deleted: able

REaster 12/28/2015 5:01 PM
Deleted: the

REaster 12/28/2015 5:01 PM
Deleted: s

Freshly emitted carbonaceous aerosols are usually hydrophobic, especially those emitted from fossil fuel combustion. They cannot serve as cloud condensation nuclei (CCN). However, these particles can experience physical and chemical ageing in the atmosphere. Condensation and coagulation processes coat carbonaceous particles with soluble species (e.g., sulfate), which enables them to nucleate cloud droplets. Inside clouds, once these cloud droplets are converted to raindrops via various rain-production processes, carbonaceous aerosols in the cloud droplets can be removed from the

atmosphere when raindrops fall to the ground (i.e., the so-called nucleation scavenging). Meanwhile, when BC is internally mixed with non-absorbing soluble materials, its absorption of sunlight can be enhanced compared to the external mixing treatment, as the soluble materials act as a lens (for the shell-core representation of particle morphology) (Jacobson 2001, 2003) or expand the cross section of the absorbing material (for the volume mixing representation) (Adachi et al., 2010). Therefore, in order to simulate aerosol concentration, spatial distribution, lifetime, and climate forcing correctly, a physically based representation of atmospheric processes affecting the mixing state of carbonaceous aerosols is needed in the models.

The simplest treatment of carbonaceous aerosols, e.g., bulk models, assumes that carbonaceous aerosols and other aerosol types (e.g., sulfate) are externally mixed (i.e., different components do not coexist in the same particle), and often uses a prescribed time scale (1-2 days) for the ageing of primary carbonaceous aerosols from the hydrophobic to hydrophilic state (Cooke and Wilson, 1996; Tie et al., 2005). More sophisticated treatments, e.g., modal and sectional aerosol models, predict the aerosol size distribution, and determine the mixing state of carbonaceous aerosols by the coating thickness of soluble materials such as sulfate and organics on these aerosols (e.g., Liu et al., 2005; Stier et al., 2005; Spracklen et al., 2005; Bauer et al., 2008). Even more advanced aerosol treatments explicitly resolve the mixing state by tracking the composition of individual particles in a population of different aerosol types (Riemer et al., 2009). However, this approach is computationally prohibitive for global models.

Liu et al. (2012) developed a modal aerosol module (MAM) for the Community Atmosphere Model version 5 (CAM5). The 7-mode version of MAM (MAM7) provides

Ghan , Steven J 12/30/2015 12:28 PM
Deleted: (Jacobson, 2001; 2003),

Ghan , Steven J 12/30/2015 12:25 PM
Deleted:

Xiaohong Liu 1/7/2016 12:00 PM
Deleted: ;

Xiaohong Liu 1/7/2016 11:59 AM
Deleted: :

Xiaohong Liu 1/7/2016 12:03 PM
Deleted: ,

Xiaohong Liu 1/7/2016 12:03 PM
Deleted: s

Xiaohong Liu 1/7/2016 12:00 PM
Deleted: :

Ghan , Steven J 12/30/2015 12:25 PM
Deleted: causing the BC particles to absorb more sunlight

138 the benchmark simulation of aerosols in CAM5. In MAM7, the microphysical ageing of
139 primary carbonaceous aerosols from the primary carbon mode to the accumulation mode
140 through condensation and coagulation is explicitly treated, with a threshold coating
141 thickness of three monolayers of sulfate. For the sake of computational efficiency, a
142 simplified 3-mode version of MAM (MAM3) was developed for use as the default in
143 CAM5. MAM3 is based on the MAM7 by merging the primary carbon mode with the
144 accumulation mode, and assuming instantaneous internal mixing of primary
145 carbonaceous aerosols with secondary aerosols (e.g., sulfate and secondary organic
146 aerosols).

147 CAM5 with MAM3 is able to simulate many features of the observed spatial
148 distribution of concentrations of different types of aerosol, aerosol optical depth, aerosol
149 number and size distribution over different geographical regions of the world. However,
150 similar to other global models (Koch et al., 2009), CAM5 significantly underestimates
151 the near-surface BC concentrations in remote regions, e.g., in the Arctic (Liu et al., 2012;
152 H. Wang et al., 2013; Ma et al., 2013a). While the underestimation of BC emission in
153 Asia (e.g., Cohen and Wang, 2014) and in the high latitudes of the northern hemisphere
154 (NH) (e.g., Stohl et al., 2013) can be an important factor, the excessively efficient
155 scavenging of BC by liquid cloud processes (H. Wang et al., 2013) and the coarse
156 horizontal resolution (~100-200 km) of the model (Ma et al., 2014) also contribute to this
157 model bias.

158 To address this low BC bias found in CAM5 with MAM3 as well as in many
159 GCMs, without significantly increasing the computational cost, we have developed a 4-
160 mode version of MAM (MAM4) for the next generation of GCMs, including the version

6 of CAM (CAM6) and the U.S. Department of Energy's Accelerated Climate Modeling for Energy (ACME).

In this paper, we provide a technical description and a first evaluation of MAM4. The paper is organized as follows. Section 2 describes MAM4. Section 3 introduces the sensitivity tests related to the microphysical ageing of primary carbonaceous aerosols and model horizontal resolution. Comparison of MAM4 with MAM3 and evaluation of MAM4 with observation data focusing on BC are given in section 4. Conclusions are drawn in section 5.

2. Model Description

2.1 CAM5

CAM5 is the atmosphere component of the Community Earth System Model version 1 (CESM1.0) (Neale et al., 2012). Compared to its earlier versions, CAM5 is designed to simulate aerosol effects on stratiform clouds (i.e., indirect effect) through acting as CCN and ice nuclei (IN). Aerosol effects on convective cloud microphysics are not treated in CAM5. MAM predicts the mass mixing ratios of internally mixed aerosol species within an aerosol mode and number concentrations of aerosol in that mode (Liu et al., 2012). A two-moment stratiform cloud microphysics scheme (Morrison and Gettelman, 2008; Gettelman et al., 2010) predicts the mass and number mixing ratios of cloud liquid and cloud ice, diagnoses the mass and number mixing ratios of rain and snow, and considers the complicated conversions among the cloud hydrometeors. The nucleation (i.e., in-cloud) scavenging of aerosols in stratiform clouds is treated consistently with the droplet activation in cloud microphysics (Abdul-Razzak and Ghan,

REaster 12/28/2015 5:03 PM
Deleted: included

2000), by explicitly calculating aerosols in the cloud-liquid-borne state (Ghan and Easter, 2006). Aerosols can affect ice microphysics by homogeneous ice nucleation of aerosol solution droplets (e.g., sulfate aerosol) in cirrus clouds with temperatures lower than about -37 ºC and heterogeneous ice nucleation in cirrus clouds and in mixed-phase clouds (Liu et al., 2007; Liu and Penner, 2005). However, aerosol scavenging by these ice nucleation processes is neglected in CAM5.

Other major components in CAM5 include (1) a stratiform cloud macrophysics scheme (Park et al., 2014) to estimate the cloudy volume (cloud fraction), (2) a moist turbulence scheme (Bretherton and Park, 2009) to explicitly simulate stratus-radiation-turbulence interactions, (3) a radiation scheme (Iacono et al., 2008) to more accurately treat the radiative effects of clouds and aerosol, (4) a shallow convection scheme (Park and Bretherton, 2009) to better simulate the observed spatial distribution of shallow convective activity, and (5) a modified deep convection scheme (Zhang and McFarlane, 1995) with the inclusion of sub-grid convective momentum transports (Richter and Rasch, 2008) and the updated closure (Neale et al., 2008).

2.2 MAM in CAM5

There are two versions of MAM available in CAM5: the default MAM3 and an optional MAM7 (Liu et al., 2012). MAM3 predicts the aerosol size distribution with three aerosol modes (Aitken, accumulation and coarse modes), while MAM7 includes seven aerosol modes (Aitken, accumulation, primary carbon, fine dust and fine sea salt, coarse dust and coarse sea salt modes). In MAM3 instantaneous ageing of primary carbonaceous particles is assumed by emitting them in the accumulation mode, while in MAM7 the ageing of the carbonaceous particles in the primary carbon mode due to the condensation

of sulfuric acid (H_2SO_4 vapor), ammonia (NH_3), and the semi-volatile organics, and the coagulation of Aitken mode particles with primary-carbon mode particles are explicitly treated. Both sea salt and dust emissions are calculated on-line and are highly sensitive to the surface wind speed. Other processes in the atmosphere affecting aerosol properties (e.g., number/mass concentration, size, density, refractive index, chemical composition) include new particle formation, gas- and aqueous-phase chemistry, dry deposition and gravitational settling, water uptake, in-cloud (nucleation) and below-cloud scavenging, and release from evaporated cloud and rain drops. There are 15 transported aerosol tracers in MAM3 and 31 in MAM7.

2.3 Development of MAM4

In this study, we developed a 4-mode version of MAM (MAM4), which includes an additional primary carbon mode on top of MAM3 to explicitly treat the microphysical ageing of primary carbonaceous aerosols in the atmosphere. As in MAM7, fresh emitted POM/BC particles are put in the newly added primary carbon mode. A criterion of 8 mono-layers of sulfate or equivalent amount of secondary organic aerosol (SOA) with the same increase in volume-weighted hygroscopicity as sulfate is required to convert POM/BC particles in the primary carbon mode to the accumulation mode. We use a value of 0 for the hygroscopicity (κ parameter) of POM from all sources. This value is more representative of POM produced from fossil fuel combustion. The hygroscopicity of POM from biomass burning source can be higher (0.06-0.30) (Liu and Wang, 2010). A non-zero hygroscopicity of POM allows in-cloud scavenging of POM/BC particles in the primary carbon mode before they are aged into the accumulation mode, and then the

REaster 12/28/2015 5:05 PM
Deleted: different

Xiaohong Liu 12/25/2015 11:27 AM
Deleted: , which

differences in the POM/BC concentrations between MAM3 and MAM7 are smaller (Liu et al., 2012). A separate treatment of carbonaceous aerosols emitted from fossil fuel versus biomass burning sources will be needed to seamlessly consider the different hygroscopicity of POM. The κ value for BC is set to 0 to reflect its hydrophobic nature.

Similarly, the refractive index for BC-containing particles changes as the particles age. The refractive index for fresh particles is the volume mean of the refractive index of the BC and POM, while the refractive index of aged particles is the volume mean of the refractive index of all components of the accumulation mode.

With the new primary carbon mode, three prognostic variables are added in MAM4 compared to MAM3: mass mixing ratios of POM and BC in the primary carbon mode and number concentration of the primary carbon mode particles, which brings the total number of aerosol tracers from 15 in MAM3 to 18 in MAM4. The other aerosol tracers and precursor gases are the same as those in MAM3. The computational cost increases by ~10% for the stand-alone CAM5 (i.e., an uncoupled atmosphere-only simulation with prescribed sea surface temperatures and sea ice) with MAM4 compared to CAM5 with MAM3. As noted in Liu et al. (2012), CAM5 with MAM7 is 30% slower than CAM5 with MAM3. Figure 1 shows the schematic of aerosol modes and associated aerosol tracers in MAM4.

3. Model Configurations and Experiments

Two sets of experiments were performed using version 5.3 of CAM (CAM5.3) with the new MAM4 (hereafter CAM5-MAM4), as listed in Table 1. The first set is to test the model sensitivity to the criterion of number of mono-layers required for the ageing of POM/BC particles from the primary carbon mode to the accumulation mode.

We conducted four experiments with the number of mono-layers set to 1, 2, 4 and 8, respectively. A higher mono-layer criterion means that a larger sulfate or SOA coating thickness is needed to age the primary carbonaceous aerosols, and thus these particles will stay longer in the primary carbon mode before converting to the accumulation mode. As noted in Liu et al. (2012), for a non-hygroscopic particle with a 0.134 μm diameter, which is the volume-mean size for BC/POM emissions, the critical supersaturation in the case of 8 mono-layers of sulfate is 0.32% based on the Köhler theory, in comparison to 0.49% in the case of 3 mono-layers. These CAM5-MAM4 simulations were conducted for present-day (year 2000) emissions and climate conditions with freely evolving meteorological fields (e.g., winds and temperature) at 0.9°×1.25° (1° hereafter) horizontal resolution for 11 years. The last 10-year results are used for analysis. For comparison, an additional experiment using CAM5.3 with the default MAM3 was performed for 11 years at the same 1° horizontal resolution. We also conducted an experiment with MAM7, which gave BC and POM results very similar to MAM4 (Figure not shown), and thus are not included in the comparison.

REaster 12/28/2015 5:09 PM
Deleted: gives very similar results of

REaster 12/28/2015 5:09 PM
Deleted: as

The second set of experiments is to test the model sensitivity to the horizontal resolution (see Table 1), since model resolution has been suggested to play an important role for the BC transport to the remote regions (Ma et al., 2013a, 2014). Four experiments were conducted at 1.9°×2.5° (2° hereafter), 1°, 0.5°, and 0.25° using the specified dynamics (SD) configuration (also known as the nudging technique) where the model meteorology is strongly constrained by an external meteorological analysis (Ma et al., 2013a, 2013b, 2015; Tilmes et al., 2015). To explore the behavior of MAM4 at higher horizontal resolution, we used the ECMWF Year of Tropical Convection (YOTC) high-

resolution (0.15°) analysis to drive the model, while aerosol emissions are the same as that in the first set of experiments. The SD configuration has been recalibrated so that the model physics properly responds to the realistic meteorology (Ma et al., 2015). This approach facilitates the direct comparison between model simulations and field campaign measurements since the simulation of aerosol lifecycle (emission, transport, and deposition) is based on a realistic climate. These SD simulations were performed from 1 November 2008 to 1 January 2010, and the one-year results in 2009 were used for our analysis. The 8-monolayer criterion was used in this set of experiments. In addition, by comparing the second set of experiments with the SD configuration to the first set of experiments with the free-running configuration (e.g., MAM4L8 versus MAM4R1), we can examine the effect of model meteorology on aerosol simulations. We also ran CAM5.3 with the default MAM3 at 1° resolution with the SD configuration for comparison.

4. Results

4.1 Comparison of MAM4 with MAM3

Figure 2 shows the latitudinal and longitudinal distributions of annual mean column burdens of BC and POM from the set 1 experiments with CAM5-MAM4, in comparison with the default MAM3. BC and POM burdens have maxima in industrial regions (e.g., East Asia, Europe, and North America) and in biomass burning regions (e.g., Central and Southern Africa, South America, Indonesia, and Siberia), but a small fraction of BC and POM is transported to the Pacific and Atlantic Oceans, and to the Arctic. In general the Southern Hemisphere (SH) high-latitudes have the lowest BC and

POM burdens. As expected, BC and POM burdens from CAM5-MAM4 simulations are much higher than those with MAM3 far from source regions. The increase in BC and POM burdens with MAM4 is most evident for the largest number of monolayers. This is more clearly seen in Figure 3, which shows the relative (percentage) differences of annual mean burdens of BC and POM between MAM4 and MAM3 for the set 1 experiments. Compared to MAM3, the global total burden increase for MAM4L1 is 10% and 16%, respectively for BC and POM, while it is 128% and 174% for MAM4L8. The largest increase occurs over the remote oceans and polar regions where the background concentrations are low (see Figure 2). An increase by up to a factor of 10 can be seen in the Arctic in the MAM4L8 case. In contrast, the increase is less than a factor of 2 (i.e., less than 100%) in the regions over the continents where the major sources are. For a larger threshold number of mono-layers, carbonaceous aerosols stay longer in the primary carbon mode, indicating a slower ageing. Aerosol particles in the primary carbon mode are subject to relatively inefficient impaction scavenging by precipitating hydrometeors but are not subject to in-cloud scavenging, which allows more POM/BC to be transported to the remote regions. We note that non-carbonaceous aerosols (i.e., sulfate, SOA, mineral dust and sea salt) are affected very little (i.e., ~1% difference for dust, and less than 0.5% difference for other aerosol species, which are about an order of magnitude smaller than their interannual variabilities) by the introduction of the primary carbon mode. The number of CCN at 0.1% supersaturation, which is important for the cloud formation and climate, changes by ~6% on the global mean.

Figure 4 shows the latitudinal and longitudinal distributions of annual mean BC and POM column burdens from the set 2 experiments. With an increase of the horizontal

REaster 12/28/2015 5:17 PM
Deleted: (while still subject to impaction scavenging by precipitating hydrometeors)

resolution from 2° to 0.25° for CAM5-MAM4 simulations, BC and POM burdens both increase by 10-20% on the global mean and by about a factor of 2 in the Antarctic. This increase is due to (1) the resolved meso-scale eddies at higher resolutions which leads to stronger poleward eddy transport of aerosol species, and (2) less frequent wet scavenging resulting from the reduced frequency of collocation between aerosols and clouds at higher resolutions (Ma et al., 2014). Figure 5 shows the percentage differences of annual mean BC and POM burdens at 1°, 0.5°, and 0.25° relative to 2° for the set 2 experiments with CAM5-MAM4. With the increase of horizontal resolution, clearly more BC and POM are transported to the remote regions. The largest increase occurs in the Antarctic by up to a factor of 2. Other strong increases are seen in regions away from major sources, such as the Arctic, western and eastern Pacific, East Asian and North American pollution outflow regions, indicating the enhanced transport out of the source regions at higher resolutions. The resolution sensitivity of BC and POM, as well as other aerosols, can contribute to the resolution sensitivity of aerosol-cloud interactions such as the enhanced but less frequent droplet nucleation due to stronger subgrid vertical velocity, reduced collocation of aerosols and clouds, and higher aerosol concentration (Ma et al., 2015). The regions with the smallest relative increases are the POM/BC source regions (e.g., East Asia, Southern Africa, South America), and the subtropical dry zones where cloud and precipitation scavenging of aerosols is relatively weak.

REaster 12/28/2015 5:19 PM
Deleted: POM/

REaster 12/28/2015 5:19 PM
Deleted: particles

By comparing MAM4L8 (in Figure 2) with MAM4R1 (in Figure 4), all else being the same, CAM5 with the one-year specific dynamics gives ~20% lower BC and POM global burdens than the 10-year free-running simulation. This can be partly attributed to the inter-annual variability of aerosols in the MAM4L8 simulation. However, the primary

cause of this difference is the different meteorological conditions between the SD and the free-running CAM5 that affect the transport and cloud processing of aerosols.

4.2 Annual global budgets of BC and POM

Tables 2 and 3 give the BC and POM budgets, respectively, for the sensitivity to the number of monolayers in the set 1 experiments. Most BC is removed from the atmosphere by wet deposition (~80%). When the number of monolayers required for microphysical ageing of BC from the primary carbon mode to the accumulation mode is increased, the contribution of wet deposition to the total BC sink decreases somewhat and the contribution of dry deposition increases. Most BC resides in the accumulation mode, indicating the relatively fast ageing of BC after it is emitted into the primary carbon mode. The ageing timescale of primary carbon mode BC (i.e., burden divided by the ageing flux from primary carbon mode to the accumulation mode) ranges from 0.24 days in MAM4L1 to 2.08 days in MAM4L8. With more monolayers and slower ageing of primary carbonaceous aerosols, more emitted BC remains in the primary carbon mode, and is not subject to cloud processing. For example, about 30% of the total BC burden is in the primary carbon mode for the MAM4L8 experiment, compared to 6% for the MAM4L1 experiment. The total BC burden increases from 0.087 (MAM4L1) to 0.123 Tg (MAM4L8), because the BC lifetime increases from 4.10 (MAM4L1) to 5.79 days (MAM4L8). Interestingly, BC burden in the accumulation mode does not change much in these simulations, because the accumulation mode BC source (from ageing) and lifetime do not change much as the ageing criterion (monolayers) changes (Liu et al., 2012).

Xiaohong Liu 12/26/2015 3:25 PM
Deleted: In particular, we find that the free-running CAM5 produces a convectively less stable atmosphere, which enhances the vertical transport of aerosols to higher altitudes where the aerosol lifetimes are longer.

Xiaohong Liu 12/26/2015 3:35 PM
Deleted: However, w

REaster 12/28/2015 5:21 PM
Deleted: ith the increase in

REaster 12/28/2015 5:21 PM
Deleted: the

REaster 12/28/2015 5:21 PM
Deleted: somewhat

Similar results can be derived for POM (Table 3), except that POM emissions are ~6 times higher, and the burdens are 7-8 times higher than those of BC in these simulations. The longer lifetime of POM than that of BC reflects different spatial and temporal distributions of POM versus BC emissions from different sources (e.g., fossil fuel and biomass burning) with respect to cloud and precipitation distributions. A higher percentage of POM is emitted from biomass burning emissions than for BC, and the biomass burning emissions tend to occur more in tropical dry seasons and boreal non-winter seasons. Also, it is assumed that POM/BC from biomass burning emissions is injected into higher altitudes (up to 6 km) and thus is subject less to wet removal by clouds, compared to the POM/BC from fossil fuel, which is emitted near the surface. The inter-annual variation of modeled BC/POM due to natural variability (i.e., BC/POM difference among different years of 10-year climatology) is quantified to be very small, as indicated by the standard deviations of BC/POM budget terms about the 10-year mean in Tables 2 and 3 for the set 1 experiments.

Tables 4 and 5 give the BC and POM budgets, respectively, for the set 2 experiments. BC and POM burdens increase by 12% and 7%, respectively, from 2° to 0.25°, with the increase occurring in the accumulation mode. The nearly invariant POM and BC burdens in the primary carbon mode with resolution indicate that the microphysical ageing of primary carbonaceous aerosols is insensitive to the resolution. This is verified by the nearly constant ageing timescales of primary carbon mode POM and BC. The accumulation mode burden increases are due to longer lifetimes for the accumulation mode aerosol (e.g., 3.38 days versus 3.95 days for BC at 2° versus 0.25° resolution). This is due to slower wet removal rates (i.e., wet deposition sinks divided by

414 burdens) at higher resolution, even though the absolute wet removal sinks are slightly
415 greater at higher resolution, and the dry deposition sinks are correspondingly slightly
416 lower. Specified dynamics (MAM4R1) reduces BC and POM burdens by 18% and 14%,
417 respectively, compared to free running (MAM4L8), with most of the decrease occurring
418 in the accumulation mode.
419
420 *4.3 Comparison with in situ observations*
421 Next, we compare the simulations with a dataset obtained during the HIAPER
422 (High-Performance Instrumented Airborne Platform for Environmental Research) Pole-
423 to-Pole Observations (HIPPO) campaigns (HIPPO 1-5) over the remote Pacific from
424 80 °N to 67 °S in January and November 2009, March/April 2010, and June/July and
425 August/September 2011 (Wofsy et al., 2011). Tilmes et al. (2015) evaluated CAM5 with
426 MAM3 against these campaigns, so in this study we focus on evaluating MAM4 results.
427 Figure 6 shows the latitude-altitude cross section of the Single Particle Soot Photometer
428 (SP2) measured BC concentrations during the HIPPO 1-5 campaigns (Schwarz et al.,
429 2013), in comparison with CAM5-MAM4 simulated BC concentrations for the same time
430 periods in the set 2 experiments. Here we only show model simulations from the set 2
431 experiments where meteorological fields from the YOTC analysis are used to drive the
432 model simulations. Note that the aerosol emissions used in this study are the present-day
433 emissions (i.e., from the year 2000), so the inter-annual variability of emissions
434 (especially for biomass burning emissions) is not accounted for. The highest observed BC
435 concentrations were in March/April 2010 in the NH mid-latitudes, resulting from strong
436 transport of BC from the East Asian continents to the Pacific (Gao et al., 2014).

Xiaohong Liu 12/26/2015 3:55 PM
Deleted: and the simulations are sampled along the flight path.

Hailong Wang 12/28/2015 3:34 PM
Deleted: We n

Observed BC concentrations in the NH were lowest in August/September compared to other seasons, consistent with the strong wet scavenging of aerosols by the East Asian monsoon precipitation in the summer. Elevated BC concentrations in the NH high latitudes (e.g., Arctic) can be seen throughout the seasons, most evident in the spring time (March/April), with the maximum BC concentrations at 3-7 km, due to the transport from the NH mid-latitudes (H. Liu et al., 2011; H. Wang et al., 2013; Ma et al., 2013; Bian et al., 2014). BC concentrations in the SH over ~50°S had a maximum in August/ September 2011, and were produced from South American and Australian biomass burning activities in the dry season. The poleward transport of BC in SH can also be seen at high altitudes over 5 km, particularly during August/September.

CAM5-MAM4 running at the four model resolutions is able to capture the maximum of BC concentrations in the NH mid-latitudes in March/April 2010. MAM4 shows a better agreement with the HIPPO measurements compared with MAM3 (Tilmes et al., 2015); however, the magnitude is still too low. This could be attributed to the underestimation of BC emissions in East Asia in the IPCC AR5 emission inventory used in CAM5 (Lamarque et al., 2010), as reported by previous studies (e.g., Cohen and Wang, 2014). We also find that the simulated aerosol layers are at higher altitudes than the observations. The maximum of BC concentrations in MAM4 is generally between 5 and 10 km, suggesting that the model still has deficiency in the treatment of convective transport and scavenging of aerosols in CAM5 (H. Wang et al., 2013). Excessive BC aloft was also found in the HadGEM3–UKCA model and was attributed to the coupling of convective transport and convective scavenging (Kipling et al., 2013). This bias is also evident in model simulations in June/July and August/September 2011. Overall, the

REaster 12/28/2015 5:25 PM
Deleted: The e

REaster 12/28/2015 5:26 PM
Deleted: in HadGEM3–UKCA

model overestimates BC concentrations in the upper troposphere. With the increase of model resolution more BC is transported to the polar regions, but increases occur primarily in the upper troposphere and lower stratosphere and is particularly noticeable in January 2009.

Figures 7 and 8 compare the modeled BC profiles from the various CAM5 simulations in set 1 and 2 experiments, respectively, with SP2 measured BC profiles during the HIPPO1 campaign over the Arctic and remote Pacific in January 2009 (Schwarz et al., 2010). It is worth noting that the 10-year average from our set 1 experiments is viewed as an ensemble mean from 10 realizations, representing the free-running model's present-day BC climatology, while the observations represent BC in specific years (which depend on the specific observations). In contrast, our set 2 experiments are nudged toward the year 2009 meteorology. The differences in BC from MAM4L8 of set 1 and MAM4R1 of set 2 are due to differences in their meteorology (winds, clouds, and precipitation), which include the differences between a 10 year average (or ensemble) and a single year, as well as the differences between the free-running model's meteorology and the nudged model's meteorology (which is very close to the reanalysis).

As seen in Figure 7, vertical profiles of observed mean BC concentrations show strong variability with latitude zones, and standard deviations of observed BC concentrations are also large. The observations show that BC concentrations increase with altitude in the SH high latitudes (60-67 °S), indicating the poleward transport of BC in the upper troposphere by the general circulation. At mid-latitudes (20-60 °N and 20-60 °S), less vertical variation is observed. In the tropics (20°S-20°N), BC concentrations

Hailong Wang 12/28/2015 3:36 PM
Deleted: -

REaster 12/28/2015 5:32 PM
Deleted: the

REaster 12/28/2015 5:32 PM
Deleted: the particular

REaster 12/28/2015 6:21 PM
Deleted: By

REaster 12/28/2015 5:33 PM
Deleted: of

Xiaohong Liu 1/7/2016 11:47 AM
Deleted: The difference between MAM4L8 in set 1 and MAM4R1 in set 2 can be attributed to the difference between the present-day climatology and year of 2009, as well as the difference of meteorology between the reanalysis and the model.

Xiaohong Liu 1/7/2016 11:45 AM
Formatted: Font:(Default) Times New Roman, 12 pt

499 increase with altitude and reach a maximum near 700 hPa, likely from biomass burning,
500 and then reduce rapidly with height. Over the NH high latitudes (60-80 °N), a steady
501 decreasing trend with height is found. All the model simulations are able to capture
502 vertical distributions of BC in the SH high latitudes as well as SH and NH mid-latitudes,
503 although the MAM4 simulations with a larger number of mono-layers (e.g., MAM4L8)
504 show too high BC concentrations in the SH high latitudes. The model simulations
505 overestimate BC concentrations in the upper troposphere in all the latitude zones, while
506 they significantly underestimate observed BC concentrations at lower altitudes (below
507 400 hPa) in the NH high latitudes. The low bias of BC concentrations near the surface in
508 the NH high latitudes is improved with MAM4, but there is still an obvious discrepancy
509 between the model simulations and observations. In addition, MAM4 predicts higher BC
510 concentrations than those from MAM3 at all altitudes and all latitude zones in the set 1
511 experiments (Figure 7). With the increase of number of monolayers required for the
512 ageing of primary carbonaceous aerosols in MAM4, modeled BC concentrations increase
513 by up to a factor of 10. The same is true for the higher BC concentrations with MAM4
514 than MAM3 for the set 2 experiments at most altitudes (Figure 8). However, modeled BC
515 concentrations from MAM3 at 1° are higher than those from MAM4 at 2° in the upper
516 troposphere and lower stratosphere. Modeled BC concentrations increase substantially at
517 these altitudes from 2° to 1°. However, the changes are much smaller from 1° to 0.25° at
518 all altitudes for all latitude zones.
519 Figures 9 and 10 compare observed BC vertical profiles from four aircraft
520 campaigns in the tropics (CR-AVE and TC4), NH subtropics (AVE-Houston) and NH
521 mid-latitudes (CARB) with simulations from the set 1 and set 2 experiments,

522 respectively. AVE-Houston, CR-AVE, and TC4 are documented in Schwarz et al. (2006)
523 and CARB is documented in Clarke et al. (2007), Howell et al. (2006), and McNaughton
524 et al. (2009). Observed BC mean concentrations show a strong reduction from the
525 boundary layer to the free troposphere in the tropics (CR-AVE and TC4) and in the
526 subtropics (AVE-Houston), while there is less vertical variation of BC concentrations in
527 the upper troposphere. For the AVE-Houston, CR-AVE, and TC4 campaigns, the model
528 experiments with different numbers of monolayers required for ageing of primary
529 carbonaceous aerosols overestimate BC concentrations in the mid- and upper troposphere
530 (Figure 9), but compare better with observations in the lower troposphere. The CARB
531 campaign in the mid-latitudes of North America in June encountered biomass burning
532 plumes, and elevated BC concentrations were observed at ~800 hPa, which are not
533 captured by model simulations using the AR5 emission inventory. The SD simulations at
534 higher resolutions in the set 2 experiments (Figure 10) do not improve the overall
535 agreement with observations, which indicates the necessity of improving the model
536 physics (e.g., aerosol processing in convective clouds) and aerosol emissions (e.g., for
537 biomass burning aerosols). The modeled BC concentrations do not change significantly
538 with different model resolutions, although there is an increasing trend with increasing the
539 resolution.

540 Figures 11 and 12 compare observed BC vertical profiles from two aircraft
541 campaigns in the NH high latitudes, ARCTAS (Jacob et al., 2010) and ARCPAC (Brock
542 et al., 2011) with the set 1 and set 2 experiments, respectively. Observed BC
543 concentrations show less vertical variations from the surface to ~300 hPa than those in
544 the tropics and NH mid-latitudes, especially in the spring. This results from the poleward

545 transport of BC from NH mid-latitudes at high altitudes. Model simulations in the set 1
546 experiments underestimate observed BC concentrations below altitudes of ~300-400 hPa
547 by 1-2 orders of magnitude, especially in spring (Figure 11). Introducing the primary
548 carbon mode with the number of monolayers increasing from 1 to 8 substantially
549 increases the modeled BC concentrations in the spring, in much better agreement with
550 observations. However, the improvement of BC simulation in the summer is less
551 substantial. The difference of BC concentrations between MAM3 and MAM4 and among
552 different MAM4 experiments is much smaller in the summer, similar in magnitude to the
553 changes in the tropics and NH mid-latitudes (Figure 9). Model simulations in the set 2
554 experiments show the increase of BC concentrations with MAM4, compared to MAM3,
555 but the increase of model resolution does not produce a significant increase of BC
556 concentrations at altitudes below ~200 hPa (Figure 12).
557 Figures 13 and 14 show the seasonal variations of observed BC surface
558 concentrations at four polar sites, in comparison with the model results from MAM4 set 1
559 and 2 experiments, respectively, along with the results from MAM3. Observed BC
560 concentrations at the three Arctic sites show a strong seasonality with higher
561 concentrations in boreal spring and winter, and much lower concentrations in boreal
562 summer (by about one order of magnitude). Observed BC concentrations at the Antarctic
563 site are lower by one order of magnitude than those in the Arctic, and the seasonality is
564 weaker and different, with highest BC concentrations in the austral spring and summer.
565 At the Arctic sites, CAM5 with MAM3 substantially underestimates the observed BC
566 concentrations, especially in winter by more than two orders of magnitude, and produces
567 an opposite seasonality to the observed one. This indicates the too efficient wet

scavenging of BC during its transport from the mid-latitudes, especially in spring and winter, since uncertainty of the emissions cannot explain these large discrepancies. CAM5-MAM4, especially with the larger number of monolayers significantly increases the BC concentrations at the Arctic sites, especially in winter, and thus improves the modeled seasonality of BC concentrations. Simulated BC concentrations also increase at the Antarctic site, but the seasonality is still wrong. Increasing the model resolution of CAM5-MAM4 results in a general increase of BC concentrations in different seasons, especially in summer at the Arctic sites, which, however, weakens the simulated seasonality.

5. Discussion and conclusions

To reduce the biases of carbonaceous aerosol simulated in CAM5, a new 4-mode version of MAM (MAM4) has been developed by adding a primary carbon mode to the default 3-mode version (MAM3), and by explicitly treating the microphysical ageing of primary carbonaceous aerosols from the primary carbon mode to the accumulation mode. The computational time increases slightly by 10%, comparing to CAM5 with MAM3. As expected, CAM5-MAM4 increases BC and POM burdens and enhances BC transport to remote regions (e.g., Arctic) due to the reduced wet scavenging of BC with more BC residing in the primary carbon mode. The increases are stronger with increasing number of hygroscopic monolayers required for the ageing of primary carbonaceous aerosols. The global burdens of BC and POM increase from 0.087 to 0.123 Tg and from 0.63 to 0.96 Tg, respectively, as the number of ageing monolayers is increased from 1 to 8. The BC and POM burdens increase by a factor of 2-10 in the polar regions, depending on the

number of monolayers. The global mean lifetimes of BC and POM increase from 4.10 to 5.79 days and from 4.62 to 7.02 days, respectively. MAM4 also predicts very similar BC and POM results as MAM7 (Figures not shown).

We also explored the sensitivity of modeled carbonaceous aerosol to the horizontal resolution of CAM5-MAM4, as previous studies suggested its importance for the BC transport to remote regions (Ma et al., 2014). The global burdens of BC and POM increase from 0.098 to 0.110 Tg and from 0.81 to 0.87 Tg, respectively, as the resolution increases from 2° to 0.25°. The lifetimes of BC and POM increase from 4.61 to 5.18 days and from 5.91 to 6.35 days, respectively. The largest relative increases in BC and POM burdens occur in the Antarctic, the Arctic, the western and eastern Pacific, and in the East Asian and North American pollution outflows. The increased resolution enhances the transport of aerosols by better resolving mesoscale eddies and the separation of aerosol plumes from clouds and precipitation (Ma et al., 2014).

Modeled BC was compared to observations obtained from aircraft campaigns and at polar surface sites. For the vertical profiles of BC concentrations, CAM5-MAM4 increases the BC concentrations at all altitudes compared to MAM3. Therefore, MAM4 improves the modeled BC in the lower troposphere, especially in the Arctic. The modeled near-surface BC concentrations at the Arctic sites have stronger increases in boreal winter and spring than in summer, which improves the modeled seasonal variation of BC concentrations. However, modeled near-surface BC concentrations in the polar regions are still lower by one order of magnitude compared to observations, even with the number of monolayers of 8 and with the model resolution of 0.25°. This points to the potential problems of emissions and/or other model processes besides the ageing of

primary carbonaceous aerosols discussed in this study. H. Wang et al. (2013) found that the wet scavenging of BC might be too efficient in CAM5 due to too high liquid cloud fraction in the NH high latitudes, based on comparison of CAM5 wet scavenging rates with those from the multi-scale modeling framework (MMF) (M. Wang et al., 2011). By modifying the treatment of liquid cloud fraction used in the aerosol activation parameterization, H. Wang et al. (2013) achieved a much better simulation of near-surface BC and other aerosol species in the Arctic compared to the standard CAM5. In addition, the aerosol emission inventories used in our simulations also likely contribute to the BC low biases in the Arctic. They neglect gas flaring emissions in and around the Arctic (Stohl et al., 2013), and they may underestimate fossil fuel emissions in East Asia (Cohen and Wang, 2014).

While the modeled BC low bias in the lower troposphere is significantly reduced in the Arctic, the overestimation of BC concentrations in the mid- and upper troposphere over the Pacific and in the tropics and subtropics of North America is exacerbated with MAM4, based on the comparisons with several aircraft campaigns. With a unified treatment of vertical transport and in-cloud wet removal in convective clouds in CAM5, H. Wang et al. (2013) significantly reduced the biases of aerosol distributions in the remote free troposphere predicted by CAM5, due to the inclusion of secondary activation and thus more efficient scavenging of aerosols in convective clouds. An ongoing joint effort between PNNL and NCAR is underway to merge the MAM4 with this unified treatment of convective transport and scavenging. A more recent improved model treatment in the resuspension of aerosols from evaporated raindrops, releasing aerosol particles to the coarse mode instead of their originating mode upon complete evaporation

REaster 12/28/2015 6:15 PM
Deleted: when comparing the

REaster 12/28/2015 6:16 PM
Deleted: at

Xiaohong Liu 12/24/2015 3:00 PM
Moved (insertion) [1]

Xiaohong Liu 12/24/2015 3:01 PM
Deleted: The MMF, which

Hailong Wang 12/28/2015 3:41 PM
Deleted: low-level

REaster 12/28/2015 6:14 PM
Deleted: cloud scavenging

REaster 12/28/2015 6:14 PM
Deleted: for the NH high latitudes

Xiaohong Liu 12/24/2015 3:02 PM
Deleted: embeds a cloud-resolving model in each climate model grid column,

REaster 12/28/2015 6:15 PM
Deleted: gaveives

Hailong Wang 12/28/2015 3:42 PM
Deleted: concentrations

REaster 12/28/2015 6:15 PM
Deleted: than simulation from

Xiaohong Liu 12/24/2015 3:00 PM
Moved up [1]: (M. Wang et al., 2011)

Xiaohong Liu 12/24/2015 3:25 PM
Deleted: forest fire emissions in Siberia and Alaska as well as

Xiaohong Liu 12/24/2015 2:50 PM
Deleted: and other developing countries

of raindrops (Easter et al., 2015, personal communication), has shown a significant impact on the vertical distribution of aerosols, including large reductions in mid- and upper tropospheric BC and POM. This emphasizes the importance of improving the representations of clouds and precipitation and aerosol-cloud interactions in GCMs.

We note that in this study, we only present the results and analysis of primary carbonaceous aerosols, especially BC, since there have been more BC measurements, and POM is co-emitted with BC. The lifecycle and global budgets of other aerosol species such as sulfate, SOA, sea salt and dust are not presented in this study, since introducing the primary carbon mode has a negligible effect on these aerosol species. This is expected since sulfate and SOA primarily reside in the accumulation mode, while dust and sea salt are mostly in the accumulation and coarse modes. Changes in modeled CCN concentrations are also small. The change in the "effective" radiative forcing due to anthropogenic aerosol-radiation and anthropogenic aerosol-cloud interactions induced by the MAM4 implementation is less than 0.1 W m^{-2} in the global mean.

Xiaohong Liu 12/27/2015 8:46 PM
Deleted: aerosol

Xiaohong Liu 12/27/2015 2:42 PM
Deleted: indirect

REaster 12/28/2015 6:17 PM
Comment [1]: What is the purpose of introducing these three acronyms in the last sentence of the paper?

Xiaohong Liu 1/7/2016 11:55 AM
Deleted: (i.e., radiative flux perturbation at the top of the atmosphere due to aerosol changes between the preindustrial and present-day times)

Code availability

The release of CESM version 1.2.0 (with CAM5.3) can be obtained at (http://www.cesm.ucar.edu/models/cesm1.2/). Code modifications for the 4-mode version of Modal Aerosol Module are available upon request by contacting the corresponding author.

Acknowledgments:

This work was supported by the U.S. Department of Energy, Office of Biological and Environmental Research, Earth System Modeling Program. The Pacific Northwest

682 National Laboratory is operated for DOE by Battelle Memorial Institute under contract
683 DE-AC05-76RL01830. The National Center for Atmospheric Research is funded by the
684 National Science Foundation.
685

References

Abdul-Razzak, H., and S. J. Ghan (2000), A parameterization of aerosol activation 2. Multiple aerosol types, *J. Geophys. Res.*, *105*, 6837-6844.

Adachi, K., S. H. Chung, and P. R. Buseck (2010), Shapes of soot aerosol particles and implications for their effects on climate, *J. Geophys. Res.*, 115, D15206, doi:10.1029/2009JD012868.

Bauer, S. E., Wright, D. L., Koch, D., Lewis, E. R., McGraw, R., Chang, L.-S., Schwartz, S. E., and Ruedy, R. (2008), MATRIX (Multiconfiguration Aerosol TRacker of mIXing state): an aerosol microphysical module for global atmospheric models, *Atmos. Chem. Phys.*, *8*, 6003–6035, doi:10.5194/acp-8-6003-2008.

Bian, H., Colarco, P. R., Chin, M., Chen, G., Rodriguez, J. M., Liang, Q., Blake, D., Chu, D. A., da Silva, A., Darmenov, A. S., Diskin, G., Fuelberg, H. E., Huey, G., Kondo, Y., Nielsen, J. E., Pan, X., and Wisthaler, A.: Source attributions of pollution to the Western Arctic during the NASA ARCTAS field campaign, *Atmos. Chem. Phys.*, 13, 4707-4721, doi:10.5194/acp-13-4707-2013, 2013.

Bond, T. C., S. J. Doherty, D. W. Fahey, P. Forster, T. Berntsen, B. J. DeAngelo, M. G. Flanner, S. J. Ghan, B. Karcher, D. Koch, S. Kinne, Y. Kondo, P. K. Quinn, M. Sarofim, M. Schultz, M. Schulz, C. Venkataraman, H. Zhang, S. Zhang, N. Bellouin, S. K. Guttikunda, P. K. Hopke, M. Z. Jacobson, J. W. Kaiser, Z. Klimont, U. Lohmann, J. P. Schwarz, D. Shindell, T. Storelvmo, S. G. Warren, and C. S. Zender (2013), Bounding the role of black carbon in the climate system: A scientific assessment, *J. Geophys. Res.*, *118*, 5380-5552, doi: 10.1002/jgrd.50171.

Bretherton, C. S., and S. Park (2009), A new moist turbulence parameterization in the Community Atmosphere Model. *J. Climate*, *22*, 3422–3448.

Brock, C. A., Cozic, J., Bahreini, R., Froyd, K. D., Middlebrook, A. M., McComiskey, A., Brioude, J., Cooper, O. R., Stohl, A., Aikin, K. C., de Gouw, J. A., Fahey, D. W., Ferrare, R. A., Gao, R.-S., Gore, W., Holloway, J. S., Hübler, G., Jefferson, A., Lack, D. A., Lance, S., Moore, R. H., Murphy, D. M., Nenes, A., Novelli, P. C., Nowak, J. B., Ogren, J. A., Peischl, J., Pierce, R. B., Pilewskie, P., Quinn, P. K., Ryerson, T. B., Schmidt, K. S., Schwarz, J. P., Sodemann, H., Spackman, J. R., Stark, H., Thomson, D. S., Thornberry, T., Veres, P., Watts, L. A., Warneke, C., and Wollny, A. G.: Characteristics, sources, and transport of aerosols measured in spring 2008 during the aerosol, radiation, and cloud processes affecting Arctic Climate (ARCPAC) Project, *Atmos. Chem. Phys.*, 11, 2423-2453, doi:10.5194/acp-11-2423-2011, 2011.

Clarke, A., et al. (2007), Biomass burning and pollution aerosol over North America: Organic components and their influence on spectral optical properties and

731 humidification response, *J. Geophys. Res*., 112, D12S18,
732 doi:10.1029/2006JD007777.
733
734 Cohen, J. B., and C. Wang (2014), Estimating global black carbon emissions using a top-
735 down Kalman Filter approach, *J. Geophys. Res.*, *119*, 307–323,
736 doi:10.1002/2013JD019912.
737
738 Cooke, W. F., and J. J. N. Wilson (1996), A global black carbon aerosol model, *J.*
739 *Geophys. Res.*, *101*, 19,395–19,409.
740
741 Flanner, M. G., C. S. Zender, J. T. Randerson, and P. J. Rasch (2007), Present-day
742 climate forcing and response from black carbon in snow, *J. Geophys. Res.*, *112*,
743 D11202, doi:1029/2006JD008003.
744
745 Flanner, M. G., C. S. Zender, P. G. Hess, N. M. Mahowald, T. H. Painter, V.
746 Ramanathan, and P. J. Rasch (2009), Springtime warming and reduced snow cover
747 from carbonaceous particles, *Atmos. Chem. Phys.*, *9*, 2481–2497, doi:10.5194/acp-9-
748 2481-2009.
749
750 Flanner, M. G., Liu, X., Zhou, C., Penner, J. E., and Jiao, C. (2012), Enhanced solar
751 energy absorption by internally-mixed black carbon in snow grains, *Atmos. Chem.*
752 *Phys.*, *12*, 4699-4721, doi:10.5194/acp-12-4699-2012.
753
754 Forster, P., Ramaswamy, V., Artaxo, P., Berntsen, T., Betts, R., Fahey, D. W., Haywood,
755 J., Lean, J., Lowe, D. C., Myhre, G., Nganga, J., Prinn, R., Raga, G., Schulz, M., and
756 Van Dorland, R: Changes in atmospheric constituents and in radiative forcing, in:
757 Climate Change 2007: The Physical Science Basis, Contribution of Working Group I
758 to the Fourth Assessment Report of the Intergovernmental Panel on Climate Change,
759 Cambridge University Press, Cambridge, New York, 129–234, 2007.
760
761 Gao, Y., C. Zhao, X. Liu, M. Zhang, and L.-R. Leung (2014), WRF-Chem simulations of
762 aerosols and anthropogenic aerosol radiative forcing in East Asia, *Atmos. Environ.*,
763 *92*, 250-266, doi: 10.1016/j.atmosenv.2014.04.038.
764
765 Gettelman, A., X. Liu, S. J. Ghan, H. Morrison, S. Park, A. J. Conley, S. A. Klein, J.
766 Boyle, D. L. Mitchell, and J.-L. F. Li (2010), Global simulations of ice nucleation
767 and ice supersaturation with an improved cloud scheme in the Community
768 Atmosphere Model. *J. Geophys. Res.*, *115*, D18216, doi:10.1029/2009JD013797.
769
770 Ghan, S. J., and R. C. Easter (2006), Impact of cloud-borne aerosol representation on
771 aerosol direct and indirect effects. *Atmos. Chem. & Phys*., *6*, 4163–4174. See
772 correction *Atmos. Chem. Phys*., *7*, 293–294, 2007.
773
774 Hansen, J. and L. Nazarenko (2004), Soot climate forcing via snow and ice albedos, *Proc.*
775 *Natl. Acad. Sci. (USA)*, *101*, 423–428.
776

Hansen, J., Sato, M., Ruedy, R., Nazarenko, L., Lacis, A., Schmidt, G. A., Russell, G., Aleinov, I., Bauer, M., Bauer, S., Bell, N., Cairns, B., Canuto, V., Chandler, M., Cheng, Y., Genio, A. D., Faluvegi, G., Fleming, E., Friend, A., Hall, T., Jackman, C., Kelley, M., Kiang, N., Koch, D., Lean, J., Lerner, J., Lo, K., Menon, S., Miller, R., Minnis, P., Novakov, T., Oinas, V., Perlwitz, J., Perlwitz, J., Rind, D., Romanou, A., Shindell, D., Stone, P., Sun, S., Tausnev, N., Thresher, D., Wielicki, B., Wong, T., Yao, M., and Zhang, S. (2005), Efficacy of climate forcings, *J. Geophys. Res.*, *110*, D18104, doi:10.1029/2005JD005776.

Howell, S. G., A. D. Clarke, Y. Shinozuka, V. Kapustin, C. S. McNaughton, B. J. Huebert, S. J. Doherty, and T. L. Anderson (2006), Influence of relative humidity upon pollution and dust during ACE-Asia: Size distributions and implications for optical properties, *J. Geophys. Res.,* 111, D06205, doi:10.1029/2004JD005759.

Iacono, M. J., J. S. Delamere, E. J. Mlawer, M. W. Shephard, S. A. Clough and W. D. Collins (2008), Radiative forcing by long-lived greenhouse gases: Calculations with the AER radiative transfer models. *J. Geophys. Res.*, *113*, D13103, doi: 10.1029/2008jd009944.

Jacob, D. J., Crawford, J. H., Maring, H., Clarke, A. D., Dibb, J. E., Emmons, L. K., Ferrare, R. A., Hostetler, C. A., Russell, P. B., Singh, H. B., Thompson, A. M., Shaw, G. E., McCauley, E., Pederson, J. R., and Fisher, J. A.: The Arctic Research of the Composition of the Troposphere from Aircraft and Satellites (ARCTAS) mission: design, execution, and first results, *Atmos. Chem. Phys*., 10, 5191-5212, doi:10.5194/acp-10-5191-2010, 2010.

Jacobson, M. Z. (2001), Strong radiative heating due to the mixing state of black carbon in atmospheric aerosols, *Nature, 409*, 695-697.

Jacobson, M. Z. (2003), Reply to comment by J. Feichter et al. on "Control of fossil-fuel particulate black carbon and organic matter, possibly the most effective method of slowing global warming", *J. Geophys. Res.*, *108*, 4768, doi:10.1029/2002JD003299.

Jacobson, M. Z. (2004), Climate response of fossil fuel and biofuel soot, accounting for soot's feedback to snow and sea ice albedo and emissivity, *J. Geophys. Res.*, *109*, D21201, doi:10.1029/2004JD004945.

Jiao, C., Flanner, M. G., Balkanski, Y., Bauer, S. E., Bellouin, N., Berntsen, T. K., Bian, H., Carslaw, K. S., Chin, M., De Luca, N., Diehl, T., Ghan, S. J., Iversen, T., Kirkevåg, A., Koch, D., Liu, X., Mann, G. W., Penner, J. E., Pitari, G., Schulz, M., Seland, Ø., Skeie, R. B., Steenrod, S. D., Stier, P., Takemura, T., Tsigaridis, K., van Noije, T., Yun, Y., and Zhang, K.: An AeroCom assessment of black carbon in Arctic snow and sea ice, *Atmos. Chem. Phys*., 14, 2399-2417, doi:10.5194/acp-14-2399-2014, 2014.

Kinne, S., M. Schulz, C. Textor et al. (2006), An AeroCom initial assessment – optical

properties in aerosol component modules of global models, *Atmos. Chem. Phys.*, *6*, 1815–1834.

Kipling, Z., Stier, P., Schwarz, J. P., Perring, A. E., Spackman, J. R., Mann, G. W., Johnson, C. E., and Telford, P. J.: Constraints on aerosol processes in climate models from vertically-resolved aircraft observations of black carbon, *Atmos. Chem. Phys.*, 13, 5969–5986, doi:10.5194/acp-13-5969-2013, 2013.

Koch, D., et al. (2009), Evaluation of black carbon estimations in global aerosol models, *Atmos. Chem. Phys.*, *9*, 9001–9026.

Lamarque, J. F., et al. (2010), Historical (1850–2000) gridded anthropogenic and biomass burning emissions of reactive gases and aerosols: methodology and application, *Atmos. Chem. Phys.*, *10*, 7017–7039.

Liu, J., Fan, S., Horowitz, L. W., and Levy, H.: Evaluation of factors controlling long-range transport of black carbon to the Arctic, *J. Geophys. Res.*, *116*, D04307, doi:10.1029/2010JD015145, 2011.

Liu, X., and J. E. Penner (2005), Ice nucleation parameterization for global models, *Meteorologische Zeitschrift*, *14*, 499-514.

Liu, X., and J. Wang (2010), How important is organic aerosol hygroscopicity to aerosol indirect forcing? *Environ. Res. Lett.*, *5*, 044010, doi: 10.1088/1748-9326/5/4/044010.

Liu, X., J. E. Penner, and M. Herzog (2005), Global simulation of aerosol dynamics: Model description, evaluation, and interactions between sulfate and nonsulfate aerosols, *J. Geophys. Res.*, *110*, No. D18, D18206, doi:10.1029/2004JD005674.

Liu, X., J. E. Penner, S. J. Ghan, and M. Wang (2007), Inclusion of ice microphysics in the NCAR Community Atmospheric Model version 3 (CAM3), *J. Climate*, *20*, 4526-4547.

Liu, X., R. C. Easter, S. J. Ghan, R. Zaveri, P. Rasch, X. Shi, J. F. Lamarque, A. Gettelman, H. Morrison, F. Vitt, A. Conley, S. Park, R. Neale, C. Hannay, A. M. L. Ekman, P. Hess, N. Mahowald, W. Collins, M. J. Iacono, C. S. Bretherton, M. G. Flanner, and D. Mitchell (2012), Toward a minimal representation of aerosols in climate models: description and evaluation in the Community Atmosphere Model CAM5, *Geosci. Model Dev.*, *5*, 709-739.

Ma, P.-L., P. J. Rasch, H. Wang, K. Zhang, R. C. Easter, S. Tilmes, J. D. Fast, X. Liu, J.-H. Yoon, and J.-F. Lamarque (2013a), The role of circulation features on black carbon transport into the Arctic in the Community Atmosphere Model version 5 (CAM5), *J. Geophys. Res.*, *118*, 4657–4669, doi:10.1002/jgrd.50411.

868 Ma, P.-L., J. R. Gattiker, X. Liu, and P. J. Rasch (2013b), A novel approach for
869 determining source–receptor relationships in model simulations: a case study of
870 black carbon transport in northern hemisphere winter, *Environ. Res. Lett.*, *8*, 024042,
871 doi:10.1088/1748-9326/8/2/024042.
872
873 Ma, P.-L., P. J. Rasch, J. D. Fast, R. C. Easter, W. I. Gustafson Jr., X. Liu, S. J. Ghan,
874 and B. Singh (2014), Assessing the CAM5 physics suite in the WRF-Chem model:
875 Implementation, resolution sensitivity, and a first evaluation for a regional case study,
876 *Geosci. Model Dev.*, *7*, 755–778, doi:10.5194/gmd-7-755-2014.
877
878 Ma, P.-L., P. J. Rasch, M. Wang, H. Wang, S. J. Ghan, R. C. Easter, W. I. Gustafson Jr.,
879 X. Liu, Y. Zhang, and H.-Y. Ma (2015), How does increasing horizontal resolution
880 in a global climate model improve the simulation of aerosol-cloud interactions?,
881 *Geophy. Res. Lett.*, *42*, 5058–5065, doi:10.1002/2015GL064183.
882
883 McNaughton, C. S., Clarke, A. D., Kapustin, V., Shinozuka, Y., Howell, S. G.,
884 Anderson, B. E., Winstead, E., Dibb, J., Scheuer, E., Cohen, R. C., Wooldridge, P.,
885 Perring, A., Huey, L. G., Kim, S., Jimenez, J. L., Dunlea, E. J., DeCarlo, P. F.,
886 Wennberg, P. O., Crounse, J. D., Weinheimer, A. J., and Flocke, F.: Observations of
887 heterogeneous reactions between Asian pollution and mineral dust over the Eastern
888 North Pacific during INTEX-B, *Atmos. Chem. Phys*., 9, 8283-8308, doi:10.5194/acp-
889 9-8283-2009, 2009.
890
891 Morrison, H., and A. Gettelman (2008), A new two-moment bulk stratiform cloud
892 microphysics scheme in the community atmosphere model, version 3 (CAM3). Part
893 I: Description and numerical tests, *J. Climate*, *21*(15): 3642-3659, doi:
894 10.1175/2008jcli2105.1.
895
896 Myhre, G., Shindell, D., Bréon, F.-M., Collins, W., Fuglestvedt, J., Huang, J., Koch, D.,
897 Lamarque, J.-F., Lee, D., Mendoza, B., Nakajima, T., Robock, A., Stephens, G.,
898 Takemura, T., and Zhang, H.: Anthropogenic and natural radiative forcing, in:
899 Climate Change 2013: The Physical Science Basis, Contribution of Working Group I
900 to the Fifth Assessment Report of the Intergovernmental Panel on Climate Change,
901 Cambridge University Press, Cambridge, UK, New York, NY, USA, 659–740, 2013.
902
903 Neale, R. B., J. H. Richter, and M. Jochum (2008), The impact of convection on ENSO:
904 From a delayed oscillator to a series of events, *J. Climate*, *21*(22): 5904-5924, doi:
905 10.1175/2008jcli2244.1.
906
907 Neale, R. B., Chen, C.-C., Gettelman, A., Lauritzen, P. H., Park, S., Williamson, D. L.,
908 Conley, A. J., Garcia, R., Kinnison, D., Lamarque, J.-F., Marsh, D., Mills, M.,
909 Smith, A. K., Tilmes, S., Vitt, F., Cameron-Smith, P., Collins,W. D., Iacono, M. J.,
910 Easter, R. C., Ghan, S. J., Liu, X., Rasch, P. J., and Taylor, M. A.: Description of the
911 NCAR Community Atmosphere Model (CAM 5.0), NCAR/TN-486+ STR, available
912 at: http://www.cesm.ucar.edu/models/cesm1.0/cam/docs/description/cam5_desc.pdf,
913 2012.

Park, S. and C. S. Bretherton (2009), The University of Washington Shallow Convection and Moist Turbulence Schemes and Their Impact on Climate Simulations with the Community Atmosphere Model, *J. Climate*, 22(12): 3449-3469, doi: 10.1175/2008jcli2557.1.

Park, S., C. S. Bretherton, and P. J. Rasch (2014), Integrating cloud processes in the Community Atmosphere Model, Version 5, *J. Climate*, *27*, 6821-6856. doi: 10.1175/JCLI-D-14-00087.1.

Quaas, J., Ming, Y., Menon, S., Takemura, T., Wang, M., Penner, J. E., Gettelman, A., Lohmann, U., Bellouin, N., Boucher, O., Sayer, A. M., Thomas, G. E., McComiskey, A., Feingold, G., Hoose, C., Kristjánsson, J. E., Liu, X., Balkanski, Y., Donner, L. J., Ginoux, P. A., Stier, P., Grandey, B., Feichter, J., Sednev, I., Bauer, S. E., Koch, D., Grainger, R. G., Kirkevåg, A., Iversen, T., Seland, Ø., Easter, R., Ghan, S. J., Rasch, P. J., Morrison, H., Lamarque, J.-F., Iacono, M. J., Kinne, S., and Schulz, M.: Aerosol indirect effects – general circulation model intercomparison and evaluation with satellite data, *Atmos. Chem. Phys.*, 9, 8697–8717, doi:10.5194/acp-9-8697-2009, 2009.

Richter, J. H. and P. J. Rasch (2008), Effects of convective momentum transport on the atmospheric circulation in the community atmosphere model, version 3, *J. Climate*, *21*, 1487-1499. doi: 10.1175/2007jcli1789.1.

Riemer, N., M. West, R. A. Zaveri, and R. C. Easter (2009), Simulating the evolution of soot mixing state with a particle-resolved aerosol model, *J. Geophys. Res.*, *114*, D09202, doi:10.1029/2008JD011073.

Samset, B. H., Myhre, G., Herber, A., Kondo, Y., Li, S.-M., Moteki, N., Koike, M., Oshima, N., Schwarz, J. P., Balkanski, Y., Bauer, S. E., Bellouin, N., Berntsen, T. K., Bian, H., Chin, M., Diehl, T., Easter, R. C., Ghan, S. J., Iversen, T., Kirkevåg, A., Lamarque, J.-F., Lin, G., Liu, X., Penner, J. E., Schulz, M., Seland, Ø., Skeie, R. B., Stier, P., Takemura, T., Tsigaridis, K., and Zhang, K.: Modelled black carbon radiative forcing and atmospheric lifetime in AeroCom Phase II constrained by aircraft observations, *Atmos. Chem. Phys*., 14, 12465-12477, doi:10.5194/acp-14-12465-2014, 2014.

Schwarz, J. P., et al. (2006), Single-particle measurements of midlatitude black carbon and light-scattering aerosols from the boundary layer to the lower stratosphere, *J. Geophys. Res.*, 111, D16207, doi:10.1029/2006JD007076.

Schwarz, J. P., J. R. Spackman, R. S. Gao, L. A. Watts, P. Stier, M. Schulz, S. M. Davis, S. C. Wofsy, and D. W. Fahey (2010), Global‐scale black carbon profiles observed in the remote atmosphere and compared to models, *Geophys. Res. Lett.*, *37*, L18812, doi:10.1029/2010GL044372.

960 Schwarz, J. P., B. H. Samset, A. E. Perring, J. R. Spackman, R. S. Gao, P. Stier, M.
961 Schulz, F. L. Moore, E. A. Ray, and D. W. Fahey (2013), Global-scale seasonally
962 resolved black carbon vertical profiles over the Pacific, *Geophys. Res. Lett.*, *40*,
963 5542–5547, doi:10.1002/2013GL057775.
964
965 Spracklen, D. V., Pringle, K. J., Carslaw, K. S., Chipperfield, M. P., and Mann, G. W.
966 (2005), A global off-line model of sizeresolved aerosol microphysics: I. Model
967 development and prediction of aerosol properties, *Atmos. Chem. Phys.*, *5*, 2227–
968 2252, doi:10.5194/acp-5-2227-2005.
969
970 Stier, P., Feichter, J., Kinne, S., Kloster, S., Vignati, E., Wilson, J., Ganzeveld, L., Tegen,
971 I., Werner, M., Balkanski, Y., Schulz, M., Boucher, O., Minikin, A., and Petzold, A.
972 (2005), The aerosol-climate model ECHAM5-HAM, *Atmos. Chem. Phys.*, *5*, 1125–
973 1156, doi:10.5194/acp-5-1125-2005.
974
975 Stohl, A., Z. Klimont, S. Eckhardt, K. Kupiainen, V. P. Shevchenko, V. M. Kopeikin,
976 and A. N. Novigatsky (2013), Black carbon in the Arctic: The underestimated role of
977 gas flaring and residential combustion emissions, *Atmos. Chem. Phys.*, *13*, 8833–
978 8855, doi:10.5194/acp-13-8833-2013.
979
980 Schulz, M., C. Textor, S. Kinne, Y. Balkanski, S. Bauer, T. Berntse, T. Berglen, O.
981 Boucher, F. Dentener, S. Guibert, I.S.A. Isaksen, T. Iversen, D. Koch, A. Kirkevag,
982 X. Liu, V. Montanaro, G. Myhre, J. Penner, G. Pitari, S. Reddy, O. Seland, P. Stier,
983 and T. Takemura (2006), Radiative forcing by aerosols as derived from the
984 AeroCom present-day and pre-industrial simulations, *Atmos. Chem. Phys.*, *6*, 5225-
985 5246.
986
987 Textor, C., M. Schulz, S. Guibert, S. Kinne, Y. Balkanski, S. Bauer, T. Berntsen, T.
988 Berglen, O. Boucher, M. Chin, F. Dentener, T. Diehl, R. Easter, H. Feichter, D.
989 Fillmore, S. Ghan, P. Ginoux, S. Gong, A. Grini, J. Hendricks, L. Horowitz, P.
990 Huang, I. Isaksen, T. Iversen, S. Kloster, D. Koch, A. Kirkevåg, J.E. Kristjansson, M.
991 Krol, A. Lauer, J.F. Lamarque, X. Liu, V. Montanaro, G. Myhre, J. Penner, G. Pitari,
992 S. Reddy, Ø. Seland, P. Stier, T. Takemura, and X. Tie (2006), Analysis and
993 quantification of the diversities of aerosol life cycles within AeroCom, *Atmos. Chem.*
994 *Phys.*, *6*, 1777-1813.
995
996 Tie, X., S. Madronich, S. Walters, D. P. Edwards, P. Ginoux, N. Mahowald, R. Zhang, C.
997 Lou, and G. Brasseur (2005), Assessment of the global impact of aerosols on
998 tropospheric oxidants, *J. Geophys. Res.*, *110*, D03204, doi:10.1029/2004JD005359.
999
1000 Tilmes, S., J.-F. Lamarque, L. K. Emmons, D. E. Kinnison, P. L. Ma, X. Liu, S. Ghan, C.
1001 Bardeen, S. Arnold, M. Deeter, F. Vitt, T. Ryerson, J. W. Elkins, F. Moore, R.
1002 Spackman, and and M. Val Martin (2015), Description and evaluation of
1003 tropospheric chemistry and aerosols in the Community Earth System Model
1004 (CESM1.2), *Geosci. Model Dev.*, *8*, 1395–1426, doi:10.5194/gmd-8-1395-2015.
1005

Wang, M., S. J. Ghan, R. C. Easter, M. Ovchinnikov, X. Liu, E. Kassianov, Y. Qian, W. Gustafson, V. E. Larson, D. P. Schanen, M. Khairoutdinov, and H. Morrison (2011), The multi-scale aerosol-climate model PNNL-MMF: model description and evaluations, *Geosci. Model Dev.*, *4*, 137-168.

Wang, H., R. C. Easter, P. J. Rasch, M. Wang, X. Liu, S. J. Ghan, Y. Qian, J.-H. Yoon, P.-L. Ma, and V. Velu (2013), Improving aerosol transport to high-latitudes in CAM5, *Geosci. Model Dev.*, *6*, 765–782, doi:10.5194/gmd-6-765-2013.

Wofsy, S. C. and the HIPPO team: HIAPER Pole-to-Pole Observations (HIPPO): fine-grained, global-scale measurements of climatically important atmospheric gases and aerosols, *Philos. T. Ser. A*, *369*, 2073–86, doi:10.1098/rsta.2010.0313, 2011.

Zhang, G. J. and N. A. McFarlane (1995), Sensitivity of Climate Simulations to the Parameterization of Cumulus Convection in the Canadian Climate Center General-Circulation Model, *Atmosphere-Ocean*, *33*(3): 407-446.

Zhang, K., H. Wan, X. Liu, S. Ghan, G. J. Kooperman, P.-L. Ma, and P. J. Rasch, D. Neubauer, and U. Lohmann (2014), Technical Note: On the use of nudging for aerosol-climate model intercomparison studies, *Atmos. Chem. Phys*., *14*, 8631–8645, doi:10.5194/acp-14-8631-2014.

Table Captions

Table 1. Model experiments. Set 1 experiments are to test the model sensitivity to the criterion of number of ageing monolayers, running CAM5-MAM4 in free-running simulations at horizontal resolution of 1°. Set 2 experiments are to test the model sensitivity to the model horizontal resolution, running CAM5-MAM4 in specified dynamics (SD) simulations with the number of ageing monolayers set to 8. In both sets of experiments the standard CAM5.3 with MAM3 is run for the comparison.

Table 2. Global BC budgets for monolayer sensitivity simulations in set 1 experiments. Numbers in parentheses are standard deviations about the 10-year mean representing inter-annual variability.

Table 3. Same as Table 2, except for POM budgets.

Table 4. Global BC budgets for resolution sensitivity simulations in set 2 experiments.

Table 5. Same as Table 4, except for POM budgets.

Xiaohong Liu 12/27/2015 8:53 PM
Deleted: of

Xiaohong Liu 12/27/2015 8:52 PM
Deleted: ning

Figure Captions

Figure 1. Schematic of aerosol modes and associated aerosol tracers in MAM4.

Figure 2. Latitudinal and longitudinal distributions of annual mean column burdens of BC (in 10^2 μg m^{-2}, left) and POM (10^3 μg m^{-2}, right) from the set 1 experiments with the default MAM3, and MAM4 with different criteria of number of monolayers (i.e., MAM4L1, MAM4L2, MAM4L4, and MAM4L8).

Figure 3. Latitudinal and longitudinal distributions of the relative (percentage) differences of annual mean burdens of BC (left) and POM (right) between MAM4 with different criteria of number of monolayers (i.e., MAM4L1, MAM4L2, MAM4L4, and MAM4L8) and MAM3 in the set 1 experiments.

Figure 4. Latitudinal and longitudinal distributions of annual mean column burdens of BC (in 10^2 μg m^{-2}, left) and POM (10^3 μg m^{-2}, right) from the set 2 experiments with the default MAM3 at 1° horizontal resolution (MAM3R1), and MAM4 at different horizontal resolutions (i.e., MAM4R2, MAM4R1, MAM4R0.5, and MAM4R0.25).

Figure 5. Latitudinal and longitudinal distributions of the relative (percentage) differences of annual mean burdens of BC (left) and POM (right) from the set 2 experiments with MAM4 at 1°, 0.5°, and 0.25° relative to 2° horizontal resolution.

Figure 6. Latitude and altitude cross section of observed and simulated BC concentrations (in ng m^{-3}) during the HIAPER (High-Performance Instrumented Airborne Platform for Environmental Research) Pole-to-Pole Observations (HIPPO) campaigns (HIPPO 1-5) over the remote Pacific from 80 °N to 67 °S in January and November 2009, March/April 2010, and June/July and August/September 2011. MAM4 simulated BC concentrations for the same time periods in the set 2 experiments at different horizontal resolutions (i.e., MAM4R2, MAM4R1, MAM4R0.5, and MAM4R0.25) are used for comparison. The model simulations are sampled along the flight paths.

Figure 7. Observed and simulated vertical profiles of BC concentrations (in ng kg^{-1}) during the HIPPO1 campaign over the Arctic and remote Pacific in January 2009. Dark solid curves are for observation means, and shaded areas for the plus/minus one standard deviation of observations. The CAM5 simulations in the set 1 experiments (i.e, MAM3, MAM4L1, MAM4L2, MAM4L4, and MAM4L8) are used for comparison. Simulated profiles are averaged over the points on the map and the indicated month of the field campaign.

Figure 8. Same as Figure 7, except for CAM5 simulations in the set 2 experiments (i.e., MAM3R1, MAM4R2, MAM4R1, MAM4R0.5, and MAM4R0.25).

Figure 9. Observed and simulated vertical profiles of BC concentrations (in ng kg^{-1}) from four aircraft campaigns in the tropics, NH subtropics and NH mid-latitudes: AVE-Houston (NASA Houston Aura Validation Experiment) in November 2010 and 2012,

respectively, CR-AVE (NASA Costa Rica Aura Validation Experiment) in February 2006, TC4 (Tropical Composition, Cloud and Climate Coupling) in August 2007, and CARB (NASA initiative in collaboration with California Air Resources Board) in June 2008. Observations are averages for the respective campaigns with dark solid curves for observation means, dark dashed curves for observation medians, and shaded areas for the plus/minus one standard deviation of observations. Simulated profiles for the CAM5 simulations in the set 1 experiments (i.e., MAM3, MAM4L1, MAM4L2, MAM4L4, and MAM4L8) are averaged over the points on the map and the indicated month of respective field campaign.

Figure 10. Same as Figure 9, except for CAM5 simulations in the set 2 experiments (i.e., MAM3R1, MAM4R2, MAM4R1, MAM4R0.5, and MAM4R0.25).

Figure 11. Same as Figure 9, except for BC profiles in the NH high latitudes from two other aircraft campaigns: ARCTAS (NASA Arctic Research of the Composition of the Troposphere from Aircraft and Satellite) in spring (April) and summer (June-July) 2008, and ARCPAC (NOAA Aerosol, Radiation, and Cloud Processes affecting Arctic Climate) in spring (April) 2008. Simulated profiles are averaged over the points on the map and the indicated month of respective field campaign.

Figure 12. Same as Figure 11, except for CAM5 simulations in the set 2 experiments.

Figure 13. Seasonal variations of observed and simulated BC surface concentrations (in ng kg^{-1}) at four polar sites. CAM5 simulations in the set 1 experiments (i.e., MAM3, MAM4L1, MAM4L2, MAM4L4, and MAM4L8) are used for comparison.

Figure 14. Same as Figure 13, except for CAM5 simulations in the set 2 experiments (i.e., MAM3R1, MAM4R2, MAM4R1, MAM4R0.5, and MAM4R0.25).

Table 1. Model experiments. Set 1 experiments are to test the model sensitivity to the criterion of number of ageing monolayers, running CAM5-MAM4 in free-running simulations at horizontal resolution of 1°. Set 2 experiments are to test the model sensitivity to the model horizontal resolution, running CAM5-MAM4 in specified dynamics (SD) simulations with the number of ageing monolayers set to 8. In both sets of experiments the standard CAM5.3 with MAM3 is run for the comparison.

Experiment Name		Mono-layer	Horizontal Resolution	Simulation Type
Set 1	MAM4L1	1	1°	Free-running
	MAM4L2	2	1°	Free-running
	MAM4L4	4	1°	Free-running
	MAM4L8	8	1°	Free-running
	MAM3	N/A	1°	Free-running
Set 2	MAM4R2	8	2°	SD
	MAM4R1	8	1°	SD
	MAM4R0.5	8	0.5°	SD
	MAM4R0.25	8	0.25°	SD
	MAM3R1	N/A	1°	SD

Xiaohong Liu 12/27/2015 9:31 PM
Deleted: of

Xiaohong Liu 12/27/2015 9:31 PM
Deleted: ning

Table 2. Global BC budgets for monolayer sensitivity simulations in set 1 experiments. Numbers in parentheses are standard deviations about the 10-year mean representing inter-annual variability.

	MAM3	MAM4L1	MAM4L2	MAM4L4	MAM4L8
Sources (Tg/yr)	7.76	7.76	7.76	7.76	7.76
Emission	7.76	7.76	7.76	7.76	7.76
Sinks (Tg/yr)	7.75 (0.008)	7.75 (0.004)	7.75 (0.007)	7.75 (0.006)	7.74 (0.006)
Dry deposition	1.30 (0.014)	1.38 (0.006)	1.42 (0.013)	1.50 (0.009)	1.64 (0.009)
Wet deposition	6.45 (0.014)	6.37 (0.008)	6.33 (0.015)	6.25 (0.011)	6.10 (0.006)
Lifetime (days)	3.95 (0.048)	4.10 (0.036)	4.30 (0.037)	4.80 (0.031)	5.79 (0.051)
Burden (Tg)	0.084 (0.001)	0.087 (0.008)	0.091 (0.0007)	0.102 (0.0007)	0.123 (0.001)
in accumulation	0.084 (0.001)	0.082 (0.007)	0.082 (0.0008)	0.083 (0.0007)	0.083 (0.001)
in primary carbon	0.000	0.005 (0.0001)	0.009 (0.0003)	0.019 (0.0005)	0.040 (0.0004)
Ageing timescale of primary carbon (days)	N/A	0.24 (0.005)	0.44 (0.015)	0.96 (0.025)	2.08 (0.02)

Table 3. Same as Table 2, except for POM budgets.

	MAM3	MAM4L1	MAM4L2	MAM4L4	MAM4L8
Sources (Tg/yr)	50.2	50.2	50.2	50.2	50.2
Emission	50.2	50.2	50.2	50.2	50.2
Sinks (Tg/yr)	50.1 (0.064)	50.1 (0.041)	50.1 (0.053)	50.1 (0.037)	50.1 (0.044)
Dry deposition	7.5 (0.086)	8.1 (0.051)	8.4 (0.061)	9.0 (0.051)	10.0 (0.049)
Wet deposition	42.6 (0.089)	42.0 (0.071)	41.7 (0.063)	41.1 (0.078)	40.1 (0.051)
Lifetime (days)	4.34 (0.049)	4.62 (0.045)	4.96 (0.038)	5.69 (0.042)	7.02 (0.095)
Burden (Tg)	0.60 (0.007)	0.63 (0.006)	0.68 (0.005)	0.78 (0.006)	0.96 (0.013)
in accumulation	0.60 (0.007)	0.59 (0.006)	0.58 (0.005)	0.59 (0.004)	0.59 (0.009)
in primary carbon	0.00	0.049 (0.001)	0.097 (0.001)	0.19 (0.004)	0.37 (0.007)
Ageing timescale of primary carbon (days)	N/A	0.37 (0.008)	0.74 (0.008)	1.48 (0.03)	2.97 (0.06)

Table 4. Global BC budgets for resolution sensitivity simulations in set 2 experiments.

	MAM3R1	MAM4R2	MAM4R1	MAM4R0.5	MAM4R0.25
Sources (Tg/yr)	7.76	7.76	7.76	7.76	7.76
Emission	7.76	7.76	7.76	7.76	7.76
Sinks (Tg/yr)	7.75	7.75	7.75	7.75	7.74
Dry deposition	1.57	2.10	2.01	1.90	1.77
Wet deposition	6.18	5.65	5.74	5.85	5.97
Lifetime (days)	3.25	4.61	4.77	5.02	5.18
Burden (Tg)	0.069	0.098	0.101	0.107	0.110
in accumulation	0.069	0.064	0.068	0.071	0.076
in primary carbon	0.000	0.034	0.033	0.036	0.034
Ageing timescale of primary carbon (days)	N/A	1.80	1.73	1.88	1.77

Table 5. Same as Table 4, except for POM budgets.

	MAM3R1	MAM4R2	MAM4R1	MAM4R0.5	MAM4R0.25
Sources (Tg/yr)	50.2	50.2	50.2	50.2	50.2
Emission	50.2	50.2	50.2	50.2	50.2
Sinks (Tg/yr)	50.1	50.1	50.2	50.1	50.1
Dry deposition	8.5	12.0	11.5	11.1	10.4
Wet deposition	41.6	38.1	38.6	39.1	39.7
Lifetime (days)	3.64	5.91	6.03	6.27	6.35
Burden (Tg)	0.50	0.81	0.83	0.86	0.87
in accumulation	0.50	0.48	0.50	0.52	0.55
in primary carbon	0.00	0.33	0.33	0.34	0.32
Ageing timescale of primary carbon (days)	N/A	2.68	2.66	2.73	2.56